Recording and quantification of ultrasonic echolocation clicks from free-ranging toothed whales

Madsen P.T.*[1,2] and Wahlberg M.[1]

1) Dept. of Zoophysiology, Institute of Biology, Build. 1131, University of Aarhus, Denmark
2) Woods Hole Oceanographic Institution, Woods Hole, MA 02543, USA

*peter.madsen@biology.au.dk

Prepared for Deep-Sea Research

Abstract

Toothed whales produce short, ultrasonic clicks of high directionality and source level to probe their environment acoustically. This process, termed echolocation, is to a large part governed by the properties of the emitted clicks. Therefore derivation of click source parameters from free ranging animals is of increasing importance to understand both how toothed whales use echolocation in the wild and how they may be monitored acoustically. This paper addresses how source parameters can be derived from free ranging toothed whales in the wild using calibrated multi-hydrophone arrays and digital recorders. We outline the properties required of hydrophones, amplifiers and analog to digital converters, and discuss the problems of recording echolocation clicks on the axis of a directional sound beam. For precise localization the hydrophone array apertures must be adapted and scaled to the behavior of, and the range to, the clicking animal, and information on hydrophone locations is critical. We provide examples of localization routines and outline sources of error that lead to uncertainties in localizing clicking animals in time and space. Furthermore we explore approaches to time series analysis of discrete versions of toothed whale clicks that are meaningful in a biosonar context.

Key words: toothed whale, ultrasound, recording, click, hydrophone, array, echolocation

Introduction

Echolocating toothed whales emit ultrasonic clicks to acquire information about their environment and to find food by reception and analysis of echoes returning from ensonified objects in the water column and the bottom (Au, 1993). The performance of a biosonar system is partly dictated by the source properties of the emitted clicks (Au, 1997; 2004) in that high amplitude signals may ensonify more distant targets and a higher directionality (figure 1A) reduces the number of unwanted echoes (also called clutter). The temporal and spectral properties of the clicks determine the information that can be derived from returning echoes. The ability to resolve the location of a target as well as its size, shape and material follow from the properties of the signal waveform (Au, 1993). A broad bandwidth of the source signal improves these abilities (Brill et al., 1992; Roitblatt et al. 1995). The detection range increases with the transmitting and receiving directionality, which in turn depends on the dominant wave lengths of the sonar signal relative to a fixed transmitting aperture. Shorter wavelengths on a fixed transmitting aperture increase the directionality both on the transmitting and receiving side. Higher frequencies reduces the incoming noise levels with masking potential (Wentz, 1962)., but will also lead to a higher absorption sound energy in the medium (Urick, 1983). Thus, there is a trade off in terms of the range, noise levels, clutter reduction and resolution for a given biosonar as dictated by the transmitted signals and the sound producing structures of the echolocating animal emitting them. For example, the source properties of sperm whale echolocation clicks with very high source levels at 15-20 kHz show that these signals hold the potential to operate in a long range biosonar system (Madsen et al. 2002; Møhl et al., 2003), whereas the low amplitude, 130 kHz clicks from small toothed whales such as harbor porpoises and pygmy sperm whales preclude anything, but use in short range biosonar systems (Au et al., 1999; Madsen et al., 2005). Source properties of echolocation clicks are also relevant for passive acoustic monitoring with towed arrays (Barlow and Taylor, 2005), sonobuoys (Levenson 1974) and automated porpoise detectors (e.g. Tpods) for optimizing detection routines and classification of species on the basis of acoustic cues.

Echolocating animals point the sound beam on the target of interest (Au, 1993), so for a meaningful evaluation of the consequences for performance of a biosonar system, it is of paramount importance that the source properties are derived for clicks on or close to the acoustic axis of the sound beam (figure 1A). It is

not only the acoustic intensity which differs greatly with the recording aspect relative to the animal, but also the temporal and frequency properties of the signal changes (figure 1A). Clicks recorded on the acoustic axis of the transmitting aperture are generally of broad bandwidth and short duration. As the recording aspect increases, the frequency content decreases, as the high frequency components are more directional than the low frequency ones. Sound does not come from a point source in the toothed whale nasal complex, but from an extended aperture of many small sources, which means that the duration of the click increases, as sound produced by various parts of the source arrives with increasing delays. For some species of toothed whales, such as porpoises, dwarf and pygmy sperm whales and dolphins of the genus *Cephalorhynchus* producing narrow band high frequency signals, these distorting effects are small (Au et al. 1999), because of the smaller potential for interference.

For on-axis measurements in captivity the animal can be trained to hold station in a hoop or on a bite plate and transmit clicks towards an array of hydrophones in front of it (Au et al., 1974). Such investigations have provided critical information on the performance of toothed whale biosonar, and have formed the basis for formulating meaningful parameters and models for emission and use of toothed whale sonar signals (Au, 1993). However, as shown for bats (Surlykke and Moss, 2000), it can be questioned if data on the transmission system from trained animals studied in captivity are representative of the signals free ranging animals produce while using their biosonar for orientation and food finding in natural habitats (Au, 1993; Au, et al., 2004, Au and Herzing, 2003, Madsen et al., 2004ab). With the exception of rare open water experiments (e.g. Au et al., 1974; Murchinson, 1980), animals in captivity are normally recorded in small tanks where their sonar signals are of much lower amplitude than those recorded in the field, and with a much lower frequency emphasis and therefore directionality (Au 1993). Secondly, housing and training of captive toothed whales is costly, rendering derivation of source properties of clicks from all toothed whale species by means of capture and training impractical at best. Accordingly, there are good arguments for quantifying toothed whale sonar signals in the wild in habitats and in behavioural settings such as foraging for which the biosonar systems have evolved.

Field recordings are logistically challenging and must often take place in challenging weather conditions and in the presence interference from other sound sources or with more than one vocally active

species present. Moreover, estimation of source parameters of directional, high pressure transients, like toothed whale clicks, from moving sources, requires multiple receivers connected to calibrated recorders with sufficient bandwidth and dynamic range to handle such signals.

The use of hydrophone arrays for bioacoustic research at sea was pioneered in the 60's and 70's by W. Watkins and W. Schevill who recorded a large number of cetacean and pinniped species (Watkins and Schevill, 1972 and others), but employed little quantitative analysis on the recordings. Later on, Møhl and coworkers (Møhl et al., 1991) used a deep vertical array of hydrophones to localize echolocating narwhals and estimate source parameters of their clicks. These studies documented for the first time that free-ranging toothed whales could generate source sound pressure levels just as high as or higher than documented for trained animals engaged in long-range target detection experiments (Au et al., 1974). It was also demonstrated that foraging free-ranging toothed whales, in analogy with echolocating bats, produced high repetition buzzes during the final stages of prey capture (Miller et al., 1995).

Up until recent years, multi-channel recorders with sufficient bandwidths were only available in the form of analogue tape recorders (Diercjks et al., 1973; Weber, 1963). Unfortunately, high speed analog recording systems have limited dynamic range and are large, expensive and cumbersome to handle. Analysis of recordings stored on magnetic tape is either hampered by the time consuming processes of analog signals analysis or often by subsequent less-than-real time digitization of the analog signals (see Watkins and Daher, 1991). Development of high speed digital recorders and PC based signal processing of discrete signals have made recording and derivation of source properties of toothed whale clicks much less expensive and less cumbersome, and therefore accessible to a larger community of researchers. The use of digital recording gear to quantify source properties of biosonar sound sources underwater is nevertheless not straightforward and researchers at sea are faced with an array of pitfalls and technical challenges in concert with questions of how to approach the analysis of directional ultrasonic sound pulses.

Here we provide a technical overview and a critical evaluation of methods to record and quantify ultrasonic echolocation clicks from free-ranging toothed whales at sea using digital, multichannel recording systems. We outline array configurations, specifications, and calibration of hydrophones and amplifiers suited for recording and localization of ultrasonic transients from toothed whales, and we discuss signal

processing approaches to provide quantitative parameters of discrete versions of toothed whale clicks. We address common pitfalls and provide recommendations that will hopefully facilitate the use of experimentally comparable approaches to areas of field-bioacoustics, biosonar research and passive acoustic monitoring.

Recording and localization

Background

Sound consists of particle motions that create a pressure wave propagating away from the sound source at a sound speed determined by the properties of the medium. A sound field is therefore made up by a particle velocity component (v) and a pressure component (p), and their product defines the acoustic intensity (I):

$$I = p \cdot v,$$

The particle velocity is given by the pressure divided by the acoustic impedance of the medium. In the acoustic free field, far from the sound source and any reflecting boundaries, the acoustic impedance is the product of the sound velocity c and the density of the medium (ρ). Under those circumstances the sound intensity may therefore be calculated as

$$I = p^2 / (\rho c).$$

Usually, we express the sound intensity in decibel units:

$$10 \log_{10} (I / I_0)$$

where I_0 is the intensity of a plane wave with an rms sound pressure of 1 µPa.

Accordingly, we quantify the sound pressure as

$$\text{dB re µPa} = 20 \log_{10} (p / p_0)$$

where p_0 is reference sound pressure of 1 μPa quantified in the same way as the measured pressure p. The pressure wave amplitude is normally decreasing in magnitude as the sound pulse propagates away from the source. The transmission loss (TL) is defined as the ratio between the acoustic intensity one meter in front of the animal (I_{1m}) to the acoustic intensity at a distance r from the animal (I_r). By transforming to logarithmic units this ratio becomes a difference instead (Urick, 1983):

$$TL = 10 \log_{10}(I_r / I_{1m}) = 20 \log_{10}(P_r / P_{1m}) = SL - RL.$$

SL is the source level, or the acoustic intensity measured at or back calculated to one meter on the acoustic axis of the animal in decibel units, $20 \log_{10} (p_{1m}/p_0)$, where p_{1m} is the acoustic pressure 1 m from the source, and p_0 is a reference pressure of 1 μPa in water. The received level (RL) is defined as $20 \log_{10} (p_r/p_0)$, where p_r is the acoustic pressure at a distance *r* from the source.

Thus, if the transmission loss is known, the source level can be derived from measurements of the received level (Urick, 1983):

$$SL = RL + TL.$$

The apparent simplicity is seductive as it contains two terms that must be interpreted with great care. First, the received level must be measured in an unambiguous way with relevance for the hearing/sonar system of the animal in question. Secondly, the transmission loss (TL) must be known. In its most basic form the transmission loss consists of two parts: geometric spreading and absorption. Geometric spreading is caused by the sound energy being distributed over an expanding surface analogous to the ever-expanding ring of a wave created by dropping a stone into the water. In a boundary-free, iso-velocity medium, the sound wave is expanding with the distance r to the sound source as if on the surface of a sphere. The surface area of the sphere is increasing by r^2, and the acoustic intensity is thereby reduced proportional to r^{-2}. This is so-called spherical spreading (or inverse square loss) where the sound intensity in decibel units decreases by $20 \log_{10}$ (r). If the sound energy is channeled between two reflective surfaces that are close together relative to the duration of the sound pulse, the sound wave is expanding as cylindrical spreading by which the acoustic

intensity decreases by 10 $\log_{10}$ (r). In many real situations, the geometric transmission loss will be in-between cylindrical and spherical for long or continuous sounds (Richardson et al., 1995). However, from a geometric calculation for ranges and bottom depths of interest here (up to 100 m range and more than 1 m away from the surface and the bottom), the spherical spreading is a reasonable approximation for the short-duration and very directional toothed whale signals (Figure 2). Nevertheless, measurements of the transmission loss of toothed whale signals in various habitats should be conducted to test this assertion, especially when recording at long ranges of e.g. sperm whale echolocation clicks.

Absorption is a complicated process caused by molecular interactions induced by the pressure fluctuations. It may be looked at as sound being lost due to friction, e.g. sound energy being transformed into heat. Absorption is highly frequency and temperature dependant, and in the frequency range of interest for toothed whale biosonars it can be approximated by (Au 1993):

$$\alpha = A\ B\ f^2 / (B^2 + f^2)\ dB / m,$$

where f is the frequency (in Herz) and the other parameters are given by

$$A = 48.83 \times 10^8 + 65.34 \times 10^{-10}\ T\ s/m$$

$$B = 1.55 \times 10^7\ (T + 273.1) \exp(-3052/(T+273.1))\ Hz$$

T = temperature in degrees Celsius

(f = frequency in kHz). For broadband signals, higher frequencies will attenuate faster than lower ones. Thus, the transmission will low pass filter the signal and thereby change its temporal and spectral structure. This is important to consider when measuring toothed whale signals at long range. Consequently, absorption can be ignored for sperm whale clicks at 15 kHz recorded at 500 meters (<1dB absorption), but must be considered for a porpoise click at 130 kHz at the same (>20 dB absorption at 500m) and much shorter ranges.

Combining geometric spreading and attenuation, the transmission loss may be quantified as

$$TL = 20 \log (r) + \alpha r.$$

This formula assumes spherical spreading, applicable within a certain range depending on the signal duration and depth of the hydrophone, sea floor and the clicking animal. On top of this, the transmission loss is affected by several other processes. A varying sound velocity of the medium will cause the sound waves to bend, very much like optical rays through a lens. This refraction may significantly affect the transmission loss at larger ranges (Lynch and Kuperman, 2003), but for distances of interest here (normally less than 100 meters, except for sperm whales) the problem is small. Sound will also be scattered by objects in the medium that are large enough relative to the dominant wavelengths of the sound to provide efficient backscatter.

Recording gear

A recording chain for underwater recordings normally consists of a hydrophone, a preamplifier,and a band-pass filter connected to a digital recorder (figure 3). The hydrophone is normally a piezo-ceramic pressure to voltage transducer that generates a given voltage (V) per Pascal (Pa) of sound pressure that is impinging on it (Lewin 1973). Given the large dynamic range of received sound pressures and the general use of the dB scale, hydrophone sensitivity is specified in dB re 1V per µPa. For example, a hydrophone with a sensitivity of -180 dB re 1V per µPa provides 1 nV per 1 µPa of sound pressure impinging on it ($20\log_{10}(10^{-9}V/1V) = -180$ dB re 1V) , and a hydrophone with a sensitivity of -200 dB re 1V per µPa would be 20 dB (10 times) less sensitive. Another way of looking at it is simply that the hydrophones will generate 1V if exposed to 180 and 200 dB re 1µPa, respectively. Hence, an output of 0.5 V (- 6 dB re 1V) from a hydrophone with a sensitivity of -180 dB re 1V per µPa means that a sound pressure of 174 dB re 1µPa (180 dB re 1uPa – 6dB) is impinging on it. Thus, the sound pressure level, *z*, impinging on a hydrophone is simply given by the voltage, *y*, in dB re 1V, plus the sound pressure, *x*, it takes to generate 1V in the hydrophone minus any gain used:

$$z \text{ dB re 1 } \mu\text{Pa} = \left|xdBre1V/\mu Pa\right| + 20\log_{10}(yV/1V) - Gain$$

The sensitivity of hydrophones is frequency dependant with a maximum sensitivity at the resonance frequency of the piezoceramic element. Generally for good hydrophones, the frequency response is acceptably flat (<±2 dB) below the resonance frequency (figure 4a). It is therefore important to use a

hydrophone that has a resonance frequency well above the frequency range of interest (figure 4a). For recording ultrasonic clicks of toothed whales, this calls for hydrophones with small piezoceramic elements, which in turn are quite insensitive (less voltage per µPa). Another argument for using a small or spherical hydrophone elements is that non-spherical hydrophones become directional when the wavelength of the sounds impinging on it is comparable to or smaller than the physical dimensions of the hydrophone element (Figure 4b,c). By using hydrophones with small spherical or cylindrical piezoceramic elements their receiving beam pattern is close to omnidirectional also at high frequencies (figure 4b,c), and can therefore be used to measure ultrasonic transients from toothed whales without correcting for directional sensitivity.

The low sensitivity of small piezoceramic elements can to some degree be countered by introducing a preamplifier next to the element as an integrated part of the hydrophone. This means that the hydrophone effectively becomes more sensitive, and that the output can be driven in long cables without having the capacitance of the element and the resistance of the cable affecting the sensitivity and the frequency response of the hydrophone. The use of small hydrophone elements means that the resulting signal to noise ratio will be poorer, and therefore such hydrophones, even with good preamplifiers, cannot be used to record natural ambient noise levels at low wind speeds (Wentz, 1962). Thus, there is a trade off between choosing small hydrophone elements for obtaining a sufficient flat recording bandwidth with omnidirectional sensitivity, and at the same time maintain an adequate signal to noise ratio in the recordings.

Hydrophones should come with specification charts stating their sensitivity as a function of frequency and direction (fig 4A). However, with or without calibration charts it is good practice to check the overall sensitivity through calibration ideally prior to and after every recording. Recording of a calibration signal through the entire recording chain and generation of a wave file with a known sound pressure level is reassuring for subsequent derivation of absolute sound measures of toothed whale clicks. Calibration can be done with a pistonphone, by insert voltage calibration, relative to a hydrophone of known sensitivity or by reciprocity calibration (Urick, 1983), but should be done in a way that ensures that the hydrophone is calibrated in the frequency range of interest.

We will not deal with analog recorders here (see Weber 1963, Diercks et al., 1971; Watkins and Daher, 1992 for use of analog tape recorders), but focus on digital recordings of high sampling rate. A digital

recorder is based on an analog to digital converter (ADC) that creates a discrete time series from an analog voltage input (figure 3). The maximum frequency, the so-called Nyquist frequency, at which a signal can be unambiguously described requires at least 2 samples per pressure/voltage cycle (the Nyquist sampling theorem), and theoretically any frequency below the Nyquist rate can be represented unambiguously. For reasons listed below, it is prudent to sample fast enough that the Nyquist frequency (sampling rate/2) is significantly higher than the highest frequency of interest.

The effective dynamic range of a recording system provides the range of resolved amplitudes that can be covered between the system noise floor and saturation (clipping). The noise floor is defined by the combination of the noise contributions from each active and resistive component in the recorder from the hydrophone up to and including the ADC and can even include quantization noise from audio compression on the digital side. Usually, however, the noise floor is dominated by one contribution, almost invariably, either the preamplifier immediately following the hydrophone or the ADC. Clipping occurs whenever the signal is too large to be represented by the voltage or digital numbers available. It too can occur anywhere in the recording circuit but is most likely to happen in the ADC. The peak-to-peak dynamic range of an ADC (i.e. the ratio of the largest signal that can be represented without clipping to the maximum quantization noise) is given by 2^N, where N is the number of bits (nbits in figure 3). For a sine-wave input, the RMS dynamic range is 2^N+3.5 dB. Each bit therefore provides 6dB of dynamic range. For example, an 8 bit ADC provides 256 quantization steps (2^8, 48 dB pk-pk dynamic range), whereas a 16 bit ADC provides 65376 points (2^{16} or 96 dB). In reality, few ADCs will achieve their theoretically dynamic range, and performance could be as much as 10 dB worse depending on other noise sources in the ADC, aliased noise due to an inadequate anti-alias filter, as well as noise coupled through its power supply and ground circuit. Nonetheless, an ADC with more bits will generally provide a larger dynamic range, which will allow the recording system to handle larger fluctuations in the received sound pressure levels without adjusting the gain settings, provided that the dynamic range is not limited by other parts of the recording chain. The price to pay for more than 8 bits is that the size of the wav file is doubled for the same sampling rate up to and including 16 bit. For example 500 ksamples/s at 8 bit generates 0.5 Mb/s per channel, whereas a 12, 14 or 16 bit ADC will generate 1 Mb/s at the same sampling rate (in the computer, 12 bits will be stored as a 16 bit

number) per channel. There are 24 bits and higher ADC's available, but these rarely offer more than 100 dB of dynamic range, i.e., an effective number of bits of 16-17 and there is little advantage in preserving the superfluous bits in most situations. If the gain setting in the recording chain is adjusted properly, it is our experience that the 80-90 dB of real dynamic range of a 16 bit ADC can handle the range, source and directionality induced fluctuations in received levels of toothed whale clicks effectively. Received levels of toothed whale echolocation clicks may in some cases exceed 200 dB re μPa which means that it is not possible to use the same 12 or 16 bit ADC with the same gain settings to make simultaneous recordings of the low ambient noise levels at ultrasonic frequencies (Wentz, 1962).

It is of paramount importance to measure the dynamic range of the entire recording chain under realistic conditions (e.g., with partly discharged batteries etc.) because limitations in the dynamic range that go undetected can lead to erroneous conclusions on the dynamics and properties of the toothed whale sound generator. For example, the received peak or peak-to-peak amplitudes of clicks recorded from an approaching toothed whale might appear to be independent range of the animal if there is clipping anywhere in the recorder. Calculating the source level of the animal from these measurements could lead to the interpretation that the animal was reducing its source level as it approached the hydrophone array by 20log(range), so-called automatic gain control (see Au and Benoit-Bird 2003 for a treatise), even if, in reality, the source level was invariant. It should be noted that it is not sufficient to look for +/- full-scale numbers in the ADC output to detect clipping although this is always a good thing to do as well. If clipping occurs before the ADC, e.g., in a preamplification stage, the flattened peaks of the signal will become rounded after passage through the anti-alias filter and so may appear as more-or-less normal clicks when digitized.

Localization of the sound source with multiple receivers requires synchronized sampling of a number of sound channels in the ADC. This can either be achieved by sharing a single high speed ADC among the channels (a process known as multiplexing) or by having multiple ADCs with each one dedicated to a single channel. The problem with a multiplexed file from N channels is that there will be a phase delay of (1/fs) x N seconds between the channels that must be compensated for when looking at time of arrival differences of the same click on different channels.

Depending on the hydrophone sensitivity and the voltage clipping level of the analog to digital converter (ADC), it may be necessary to amplify the hydrophone output before digitization. This is normally done in an external conditioning box with variable gain and filter settings. If the hydrophone is without a built-in preamplifier, the conditioning box should have a suitable high input impedance to avoid unwanted high pass filtering of the signal (see below) and a low output impedance to avoid attenuation when coupled to the ADC. Before digitization, a band pass filter is necessary. Low frequency noise must be reduced to avoid saturating the recording system. If signal components above the Nyquist frequency (sampling rate (fs)/2) are not filtered out, energy at frequencies above the Nyquist frequency will be folded back during digitization creating aliasing ambiguity and noise. For recording of ultrasonic clicks from toothed whales, a high pass filter at 1 kHz is often suitable. If there is no preamp built in to the hydrophone, a one pole (-6 dB/octave) high pass filter can be made in the conditioning box simply by choosing its input impedance properly. Given a hydrophone with a capacitance C (provided by the manufacturer), and a desired -3 dB cut off frequency of the filter of f_0, the input resistance of the conditioning box should be $R = 1/(2\pi f_0 C)$. The anti-alias low pass filter should be located as close as possible to the ADC to avoid picking up high frequencies in the cables between filter and ADC. It is tempting to use a steep, high order anti-aliasing filter to maximize the usable bandwidth below the Nyquist frequency while still filtering the frequencies above the Nyquist frequency efficiently, but that can cause ringing, dynamic range limitations and phase matching problems. These difficulties are substantially avoided by using a lower order (e.g., a 4-6th order Butterworth)_low pass filter that starts well below the Nyquist frequency. A good rule of thumb is to sample at least three times faster than the highest frequency of interest. For some toothed whale signals a bandwidth of 150 to 200 kHz would be required, which in turn calls for a sampling rate of 500-600 ksamples/s per channel to avoid aliasing problems. An elegant way to address aliasing problems is to use a sigma-delta converting ADC. This type of converter, common in modern audio recording equipment and PCs, samples at a very high rate and then combines samples digitally to reduce the sampling rate using a steep digital anti-alias filter.

Acoustic localization and array configurations

Localization of a vocalizing animal is important in many studies. One way to accomplish this is to record the sound of the animal with an array of receivers (Figure 5). A signal emitted by the source will arrive at the various receivers with different time delays, due to different propagation path lengths from the source to the receivers. For a certain source location relative to the array, there will be a certain set of time delays. It is possible to use these time lags to calculate the location of the source, and thereby the spatial relationship between the source and the receivers needed to estimate the transmission loss.

Consider first the problem of localizing a sound source in a 2-dimensional situation (Fig. 5). From each pair of receivers the signal time of arrival difference (TOAD) can be measured. Each such TOAD restricts the possible location of the source to a hyperbolic curve, having its axis in the direction of the line connecting the two receivers. With one more receiver, another hyperbolic curve can be generated, and the source is ideally restricted to the intersection of the two curves.

Adding the third receiver will actually add *two* hyperbolic curves, as there will be two TOADs generated by the additional reception of the click, one relative the first and one relative the second receiver. However, it follows that one of these TOADs will be a function of the other one, and provide no new information in on sound source location.

While horizontal 2-dimensional localization may be feasible for some terrestrial situations, it is usually not feasible for toothed whales moving in a 3-D world (Wahlberg et al., 2001). For localization in three dimensions, each TOAD restricts the source to a hyperboloid surface. Using the line of argument as in the 2-D example above, three such surfaces are needed to restrict the source ideally to one point. Thus, three receivers are needed to pinpoint the source location in two dimensions, whereas four receivers are needed in three dimensions. In some source-receiver constellations there may be two source locations generated by each set of TOADs, and here an extra receiver is needed to resolve the ambiguity (Spiesberger 2001).

It is important to realize that if only a minimum number of receivers are used, there will be no explicit information available on how well the localization system performs. The hyperbolas or hyperboloids will *always* (except for some pathological cases) render a single and therefore at first glance a precise result (a

perfect intersect), independent of the error in data fed to the localization algorithm. The situation is similar to the one using only two Cartesian data points to determine the slope of a line. Using linear regression the line will perfectly intersect the two data points. However, we will have no chance of knowing how accurate the determined slope is. This can only be achieved from increasing the number of data points. Similarly, more receivers are needed to determine how well the hyperboloids intersect. A well-defined intersect from many hyperboloids provides considerably more confidence in the derived source location, compared with only having one such intersect. The drawback of this is that more receivers are needed, adding logistical challenges in the field and more data to process.

The precision in the calculated source location is depending on the information fed into the localization algorithm. For good localization, precise information is needed on the receiver locations, the TOADs and the sound velocity of the medium. The meaning of 'good' and 'precise' is determined by how accurate the investigator needs to know the location of the vocalizing animal. For smaller arrays (e.g. Au et al., 2003, Schotten et al. 2004, Madsen et al., 2004), inter-receiver locations may be obtained with a measuring rod, and channel synchronization is obtained from connecting all receivers to the same recorder. For large arrays, the receiver locations may be deduced using signals emitted at known locations (Watkins and Schevill 1972, Wahlberg et al. 2001). Nowadays, the Global Positioning system has added an elegant way in which 2-D receiver locations and synchronization may be obtained from an arbitrary number of receivers located at any distance from each other (Møhl et al. 2001).

Many toothed whale species forage at great depths, and biosonar signals may not be recordable from individuals close to the surface. To perform recordings at the depths where the animals are using their biosonar, hydrophone arrays may need to be deployed at great depths. This poses some problems for the hydrophone array design (see Moehl et al., 2003; Heerfordt et al, in press) and the means by which they are deployed.

In Table I different array configurations are outlined, rendering different number and kinds of source coordinates relative the receivers of the array. In general, the more receivers that are used, the more information can be obtained about the source location. Besides outlining the number of receivers required, Table I also shows that the geometric arrangement of the receivers is critical for the localization information

that can be derived. In general, optimal source location is obtained for array distances of the same order of magnitude as the source-to-array distance, and for sources 'within' the array, or in the direction perpendicular to the array's geometric extension. For source level estimates, only the range from the receivers to the source is actually needed, and therefore a vertical linear array of sufficient aperture will do (e.g. Møhl et al., 1991, Madsen et al. 2004, Heerfordt et al, in press). Linear sparse arrays are favorable in the sense that the region of accurate localization extends quite far out from the array on its broadside axis. However, if information is also needed on animal movement and the directionality of the signals, a planar array may be more useful (e.g. Au et al., 2001; Rasmussen et al. 2004).

Additional 'virtual' hydrophones may be constructed by using surface reflected source to receiver paths that can improve the vertical resolution of the localization. In calm waters, the surface reflected path to the hydrophone may be viewed as a signal reaching a receiver situated *above* the water surface at a height corresponding to the hydrophone depth. Additional reflexions on the bottom, surface-bottom et cetera may give even more virtual hydrophones. Thereby, hyperboloids can be generated from such reflections so that the location of the whale can be estimated from single-hydrophone recordings (e.g. Aubauer et al., 2000; Laplanche et al., 2004). Likewise, hyperboloids from virtual hydrophones can be used to improve the localization precision with multi-hydrophone arrays (Møhl et al. 1991, Wahlberg et al. 2001, Thode et al. 2002).

The location of the 'virtual hydrophones', and thereby their usefulness, is critically dependent on surface waves which may disturb the perfect mirroring of the sound path, and stability in hydrophone depth (Urick, 1983). Another issue with surface-reflected paths is that, as noted below, if the animal is pointing its beam upwards so that the surface reflected path is much stronger than the direct path, we may easily misinterpret the reflected path as being the direct one. For MINNAs there is no easy way to mediate such errors. For ODAs the problem is usually quite easily recognizable as it often results in one or several hyperbolas pointing towards a completely different point of intersection than most of the other ones. Almost any one working with sound localization of whales has experienced having flying whales or whales localized below the ocean floor. Such errors can be caused by an erroneous interpretation of click multipaths or by tilt in an assumed vertical array. Such obvious errors should be regarded as an excellent chance both to control

and debug the localization algorithms used, but also to carefully scrutinize the interpretation of the recorded signals.

The coordinates of the source relative the receivers may be derived from the hyperbola intersects or through calculations. It is prudent to do both and only trust localizations, where the two independent methods render comparable results. For 3-D localization the hyperboloid plots can be projected on the vertical plane crossing one of the receivers and the best hyperboloid intersect (see Wahlberg et al. 2001).

For calculating the source location, different approaches may be used. Most of them rely on the following basic scheme. Each signal impinging on a hydrophone results in an equation which we write as

$$|\mathbf{r}_i-\mathbf{s}|^2 = (c\ T_i)^2$$

In this equation, $|\mathbf{r}_i-\mathbf{s}|$ is the distance between the source ($\mathbf{s}$) and the i:th hydrophone ($\mathbf{r}_i$). Bold types denotes vectors, so the source has coordinates $\mathbf{s} = [s_x,s_y,s_z]$, where the last element is omitted in 2-D cases. Similarly, each receiver has coordinates $\mathbf{r}_i = [r_{ix},r_{iy},r_{iz}]$, where we again omit the last element in 2-D applications. The sound velocity is denoted *c*, and T_i is the time it takes the signal to travel from the source to the receiver. There will be a total of N such equations, where N is the number of receivers in the array.

When recording signals with an array, we may determine the receiver locations and the sound velocity, but we do not know the time of arrivals, T_i. What is known, however, are the time-of-arrival differences (τ_i) between any receiver and e.g. receiver no. 1. If the first equation is subtracted from the N-1 other equations, and if we choose the coordinate system so that the first receiver is in the origin (0,0,0), we end up with the following set of equations:

$$2\ \mathbf{r}_i\,\mathbf{s} + c^2\ \tau_i\ T_1 = -\ c^2\ \tau_i^2 + |\mathbf{r}_i|^2\ ,\ i = 2\ ..\ N.$$

For MINNA systems this equation may be solved for sx, sy and sz through elimination, rendering the source coordinates. For ODA systems there will be more equations than unknowns, and least-squares or other smoothing techniques may be used to derive the source location (see Wahlberg et al. 2001 and Spiesberger 2001 for details). Another, and sometimes more reliable approach, for ODA systems is to split up the

localization system into smaller MINNA 'cells', and derive an averaged source location from the MINNA locations (Spiesberger and Wahlberg 2002, Wahlberg 2003, Spiesberger 2005).

As noted above and in Table I, different array geometries will render different numbers and types of source coordinates, and with a precision depending on many factors. For measurements of the source properties of toothed whale echolocation signals we find the linear and star-shaped arrays particularly useful. The linear array has the advantage of being able to cover a relatively large volume of the water within which it can localize sound sources with adequate precision. Three hydrophones are needed to derive the bearing and range to the sound source, which is sufficient for assessing the transmission loss and thereby the source level. Adding an extra hydrophone improves the reliability in the derived source location and thereby increases the effective range of the array. The distance between the hydrophones should be kept as large as possible, but not larger than the same signal can be recorded on all receivers. Also, the larger the inter-receiver distances, the more difficult it is to keep track of the inter-receiver distance, and the general shape of the array unless differential GPS is used for each recording station.

A disadvantage with the linear array is that it is not possible to estimate the animals' 3-D swimming direction using consecutive clicks and thereby test if the animal's body axis is generally pointing towards a hydrophone. A star-shaped array is more suited for this (Au et al.2003; Rasmussen et al. 2004). The localization algorithm and the on-array-axis localization accuracy for a star-shaped array have been published by Aubauer et al 2001. The drawback with this array type is that animals can only be localized with some confidence within a relatively narrow volume of water right in front of the array aperture. Also, most small planar arrays are MINNA systems that ideally should be augmented by an additional hydrophone to improve the confidence in the derived locations.

The localization precision will critically depend on the degrees of freedom given by array shape and size, the source-receiver geometry, the signal type and the signal-to-noise ratio (SNR). Before determining which array is needed for what kind of signal at which range, it is important to consider the required accuracy. For source level measurements of interest here, a precision within a decibel is rarely crucial. As noted above it is above all the transmission loss estimates that determine the accuracy at which the source level can be computed. For spherical spreading with an attenuation no higher than that for harbour porpoise

signals (0.038 dB/m), a variation of 2 dB in transmission loss (and thereby in source level) corresponds to a maximum absolute error in range of about 20% out to a distance of 100 m (sloping dotted line in Fig. 6). The slopes of the lines are the effect of attenuation. All toothed whales known up to date have a lower center frequency than harbour porpoise clicks, and the signals will accordingly suffer from the same or less attenuation. The biosonar signals with lowest frequency emphasis known is generated by the sperm whale, having an attenuation of about 1-2 dB/km at 15 kHz. The effect on the transmission loss of sperm whale signals is also depicted in Fig. 6 as the almost horizontal lines. All other known toothed whale clicks will be found within the 'V' of the harbour porpoise and sperm whale data.

Having determined the ranging accuracy needed, we may determine which array configuration is needed using error modeling. Such modeling can be done with many different techniques such as linear error propagation modeling (Wahlberg et al. 2001) or numerical modeling (Spiesberger and Wahlberg 2002). Numerical modeling is usually rendering the most reliable results (Spiesberger and Wahlberg 2002, Wahlberg 2003). Note that source localization precision is not only a function of the range to the receiver, but also to the source's aspect to the array (figure 7). Conveniently, another nice feature with the linear array is that it will provide robust bearing estimates so that sources located close to the array axis may be extracted for further analysis with a high degree of confidence.

Needless to say, it is clear that acoustic localization is a rather complicated process producing a large number of possible error sources for wrongly assessing the range between the whale and the receivers. It is therefore detrimental that both algorithms and hardware are regularly checked through calculating the location of sound sources produced at known locations around the array.

Analysis of array data

Array data can be used to track and monitor vocalizing animals for use in behavioral and abundance studies (e.g. Wahlberg, 2002, others). Here we will address how array data from a calibrated hydrophone array can be used to derive source parameters of echolocation clicks from toothed whales. Having obtained array recordings, the signals may be localized with some precision and the transmission loss and source level can be determined. The derived levels will most likely vary tremendously for two reasons. First, toothed

whale echolocation signals are highly directional, with a 3 dB beam width in some species smaller than ±5 degrees (Au 1993). Therefore, depending on whether the receiver is aligned with the animals' acoustic axis, the received sound level may vary by more than 40 dB. Also, animals are known to vary their apparent source level by more than 20 dB in a single click train (Madsen et al. 2002).

This poses a problem since we wish to record the on-axis source level of the clicks when assessing the sonar potential of the clicks. However, from merely inspecting the back calculated sound pressure level to one meter from the source, we have no way of telling a faint on axis signal from a powerful off-axis one. Off-axis signals may be relevant for passive acoustic monitoring, but have little value when evaluating the performance of toothed whale biosonar systems, and recording of clicks at varying degrees off-axis can lead to erroneous classification of sonar signals from the same species or animal into different click types, that may in fact to caused by varying degrees of off-axis distortion. Biosonar signals must therefore be recorded on or close to the acoustic axis of the transmitting aperture of the clicking toothed whale to quantify the clicks with respect to performance of the biosonar system and to render inter- and intra specific comparisons and classifications meaningful. Statistical treatment of clicks in the light of biosonar performance only makes sense for on-axis clicks. Subsequently, simultaneous recording of off-axis versions of the same click recorded on-axis can provide an array of useful information of the sound generating system, but only in conjunction with the on-axis version of the click.

Acknowledging these problems, the concept of the Apparent Source Level (ASL) was introduced by Møhl et al (2000) (see figure 1). The ASL is defined as the back calculated acoustic intensity 1 m *in any direction* from the sound source. While this does not facilitate classification of on-axis signals, it provides a way to report the acoustic level back-calculated to 1 m, without knowing exactly in which direction relative to the sound source the signal was recorded. The term source level (SL) should only be used for sound pressure levels back-calculated to one meter on the acoustic axis of the animal (Urick, 1983). Quite often in the bioacoustic literature source levels are reported where it would be more appropriate to use the ASL instead.

Several criteria have been used to determine whether or not a signal is recorded on axis. First, the relative amplitude difference between clicks recorded at the various receivers may be used to define the on

axis clicks as signals of highest amplitude as compared to adjacent receivers (Au et al., 2004) or within a certain amplitude difference, such as 3dB, compared to the same click on other receivers (Au and Herzing, 2003). This criteria is only useful for clicks recorded within a distance where there will be a measurable reduction in received level due to directionality on adjacent hydrophones. The amplitude information in a click train, both within the same receiver channel and adjacent ones, can be used to define on axis signals as the one with the highest back calculated sound pressure level, assuming that the animal sometimes scans the sound beam across the receivers and ensonifying one of them with its on-axis signal (Madsen et al. 2003). The latter approach can be used in conjunction with a threshold for ASL that is considered to be high enough to represent an SL (Møhl et al., 2000, 2003), but that will inevitably introduce a bias of only quantifying clicks with high source levels (Møhl et al., 2003). Surface reflections may be used to improve the confidence that the analyzed signal is on axis. If the surface reflexion has higher amplitude than the direct path, there is reason to believe that the animals acoustic axis is not pointing towards any of the receivers (Madsen et al. 2004).While the equal levels approach likely is too generous by accepting upwards 2/3 of all recorded clicks as being on-axis (Au et al., 2004), it is also clear that a minimum level approach will exclude many low amplitude clicks recorded on-axis (Møhl et al., 2003).

For broadband signals (as are most toothed whale clicks) the spectral and temporal properties give additional clues to whether or not the signal is recorded on axis (Au ref, Madsen et al., 2004; Beedholm and Møhl 2006). The acoustic localization information from tracking the animal in a series of clicks may also hint to when the acoustic axis is most likely pointing towards the array, assuming that its acoustic axis is identical to the animal's body axis as expressed by the pointing vector of the swimming direction and that localizations are accurate enough to derive a reliable velocity vector (Rasmussen et al. 2004). Irrespective of the technique used to determine if a signal is on axis, it is important to stress that no technique so far developed seems completely satisfying and none of the methods have been thoroughly ground thruthed under controlled conditions. Accordingly there is always a risk of including off axis clicks or excluding on axis clicks in the analysis. We recommend to use several of the above mentioned criteria and to be very specific about the implemented methodology and its caveats when reporting and discussing the data.

Analysis of discrete signals

This section attempts to address how the source parameters of clicks can be analyzed on the basis of discretely sampled amplitude values in a way that is meaningful for quantifying the sound generator in a biosonar system. An analog to digital recorder (ADC) creates a discrete time series by sampling amplitude values of an analog voltage signal. The sampling rate (fs) defines how often the analog signal is sampled per second. The faster the sampling rate, the higher the frequencies that can be reproduced unambiguously (see Nyquist sampling theorem above). Time and frequency domains are linked via the Fourier transform and both approaches are useful to quantify when assessing the performance and properties of toothed whale biosonar (Au, 1993; Au, 2004). In the time domain, relevant parameters include click repetition rates, sound pressure and energy measures, and duration. In the frequency domain measures of frequency emphasis and bandwidth should be computed.

A) Amplitude and duration measures

An often used proxy for the maximum range at which the toothed whale is acoustically searching for prey is the interclick interval (ICI), because toothed whales in captive trials normally use ICI's longer than the two-way travel time to the target (Au, 1993). Although the ICI may reflect the maximum time an echolocating toothed whale is prepared to wait for a returning echo, the actual two-way travel time to the target may be much longer for animals echolocating in the wild (Madsen et al., 2005). The short durations and well defined onsets of clicks make derivation of ICI straight forward and any click detector or measures by hand would normally suffice. If the time-bandwidth product (duration times bandwidth) of the signal is sufficient, higher temporal resolution in ICI's can be achieved by using a high SNR on-axis click from the same recording as a matched filter.

An absolute dB measure must be accompanied by a reference value along with information on how the magnitude of the sound pressure was quantified. Measures of magnitude for aquatic biosonars are due to lack of standardization variously reported in terms of peak-peak, peak-equivalent RMS, RMS and energy flux density measures (Au et al., 1974; Møhl et al., 1990; Au, 1993; Madsen et al., 2004). For the same transient waveform, levels in decibels may vary by 15 dB or more between different measures of pressure, rendering

meaningful comparisons difficult without detailed information about how the pressure amplitude was quantified. For a pure sine wave the ratio between peak-peak and rms is 9 dB, but for a-periodic signals, such as toothed whale click, the difference between peak-peak and RMS varies widely and can be 15 dB or more. The most common and straight forward measure for quantifying the magnitude of toothed whale clicks is the peak-peak sound pressure level (Au et al., 1974; Au, 1993), that can be read directly from an oscilloscope. However, since the mammalian ear operates as an energy detector, it is also relevant to include the rms and energy flux density measures of biosonar signals (Au et al., 1999).

A peak to peak sound pressure level can be derived in a straight forward manner from a digitized version of the click (figure 8) provided that the sensitivity, the gain of the recording chain and the maximum peak voltage of the ADC are known. Let us consider a transient from a delphinid toothed whale (figure 8a). It is impinging on a hydrophone with a sensitivity of -206 dB re. 1V/µPa and is amplified by 20 dB before digitization by an ADC with a peak clip voltage of ±5V. It follows that a 1V input to the ADC from the hydrophone and amplifier corresponds to a received sound pressure of 186 dB re 1µPa. An amplitude of unity (+1 or -1), corresponding to 5V into the ADC, in the discrete version of the click after digitization in the ADC must therefore equal a received sound pressure of 200 dB re 1µPa (peak) on the hydrophone (206 dB re 1µPa/V - 20 dB + 20log(5V/1V)). It follows that a peak to peak amplitude from the discrete signal of 1.57 (0.78 + 0.79 in figure 8d) is equivalent to a peak to peak sound pressure level of 20log(1.57) + 200 dB re 1µPa = 204 dB re 1µPa (pp).

To approximate the rms value of a click, Møhl et al. (1990, 2003) used the peak equivalent rms (perms) measure that compares the peak pressure of a click with the rms measure of the calibration signal. The perms is still a peak measure and is by definition 9dB less than the peak to peak pressure. True rms measures of toothed whale clicks will depend on the size of the chosen window over which the squared pressure is averaged. This will almost always render values higher than 9 dB, and we strongly advocate calculation of the rms sound pressure rather than using the perms measure as a proxy for rms.

The root of the mean of the squared pressure (RMS) of a plane wave in a time window from 0 to T is given by:

$$p_{rms} = \sqrt{\frac{1}{T}\int_0^T p^2(t)dt} \qquad dB\ re.\ 1\mu Pa\ (rms) = 20\log\sqrt{\left(\frac{1}{T}\int_0^T p^2(t)dt\right)}$$

[p(t) = instantaneous pressure] (Urick, 1983)

The RMS of a discrete signal with an amplitude variable *s* is computed as follows:

$$10\log\left(\frac{1}{N}\sum_1^N s^2\right)$$

The length of the analysis window is critical for RMS measures of transient signals, since the duration determines the window over which the pressure squared should be averaged (Madsen, 2005). For the same transient waveform, the rms level will decrease with increasing duration of the averaging window. Various techniques have been used to define the averaging window for toothed whale clicks. The so-called D duration, which is given by the –10 dB end points relative to the peak of the envelope of the waveform, has been applied to determine the durations of narwhal clicks (Møhl et al., 1990). The envelope is computed by taking the absolute value of the analytical signal (consisting of the signal as its real part, and the Hilbert-transformed signal as its imaginary part, Randall, 1987). As a variation of this approach, Møhl et al. (2003) used –3 dB end points relative to the peak of the envelope when computing rms measures of p1 pulses in sperm whale clicks. However, the use of the -3dB definition will render 2-3 dB higher rms measures than any other approach (Madsen, 2005) since only the highest amplitude values of the clicks are considered. We advocate either using the D-duration or a window enclosing a fixed proportion of the energy of the click, as both measures render about the same rms values (±1 dB) for good signal to noise ratios (Madsen, 2005). In the latter approach, the duration of transients is determined by using the relative energy in a window that incorporates the entire signal waveform along with short samples of noise on either side. For short duration, high SNR clicks from toothed whales a 95 or 97% energy approach has been implemented (Au, 1993; Madsen et al., 2004) (figure 8c). For example, for a 95% energy window, the onset of the signal would be

defined as the time at which 2.5% of the signal energy is reached, and the termination of the signal is defined as the time at which 97.5 % of the signal energy was reached. Using this method we find that the click depicted in figure 8a has a duration of 16 μsec compared to 17 usec derived with the -10 dB re peak of envelope approach. For very short clicks lasting few samples, it may be necessary to interpolate to achieve a better resolution (Madsen et al., 2004).

For the click of figure 8a, the rms amplitude of the waveform in the window making up 95% of the relative energy is computed to be 0.32 (figure 8d). Hence, the received rms sound pressure level can be calculated to be 20log(0.32) + 200 dB re 1uPa = 190 dB re 1uPa (rms). There is typically a difference of 13-15 dB between the rms and the peak-peak pressure of most toothed whale clicks (Au, 1993; Madsen et al., 2004).

The energy of a sound pulse is given by the intensity integrated over the pulse duration, and the intensity is proportional to the time-averaged pressure squared for a plane wave in an unbounded medium (Urick, 1983, Au, 1993). Hence, the energy flux density (dB re. 1μPa^{2}s) of transients can be approximated by 10log to the time integral of the squared pressure (sum of squared pressures for the discrete version of the signal) over the duration of the pulse (Young, 1970), which for the same duration, T, is the rms level (in dB) + 10log(T):

$$\textit{Energy flux density (dB re. 1}\mu\textit{Pa}^2\textit{s)} = 10\log\int_0^T p^2(t)dt = 10\log\left(\frac{1}{T}\int_0^T p^2(t)dt\right) + 10\log(T)$$

[T, window length in seconds]

Accordingly, we can compute the received energy flux density of the click in figure 8 by integrating the rms sound pressure over the signal duration:

190 dB re 1μPa (rms) + 10log(22 x 10^{-6} sec) = 143 dB re. 1μPa^{2}s.

The energy flux density on a dB scale (dB re. 1μPa^{2}s) can be converted to Joule/m^2 by dividing the squared pressure on a linear scale by the specific impedance Z (sound speed x density) of the medium. E.g. 143 dB re. 1μPa^{2}s = (14 Pa$_{rms}$)^{2}s / (1500 m/s x 1040 kg/m^3) = 0.13 mJoule/m^2. Subsequently, the estimated ASL or SL can be generated by adding the transmission loss (TL = 20 log (r) + αr) to the received levels computed above. E.g. if the dolphin was 12 meters from the array and the click had the energy centered around 100 kHz, the SL would be:

204 dB re 1uPa (pp) + 20log(12m) + 12m*0.03dB/m (absorption at 100 kHz) = 226 dB re 1uPa (pp). For the click in figure 8 this corresponds to SL's of 212 dB re 1uPa (rms) and 165 dB dB re. 1μPa^{2}s (20 mJoule/ m^2).

B) Frequency domain

The spectral properties of a digitized click can be quantified with the Discrete Fourier transform that links the time and the frequency domains of a signal. The most efficient calculation of a DFT is the Fast Fourier Transform (FFT), which can be used if the signal length (in samples) is a multiple of 2. The frequency resolution of an FFT-derived spectrum is given by the sampling rate (fs) divided by the FFT size. Thus, a 256 FFT on a click sampled at 500 ksamples provides a frequency bin width in the spectrum of 1.95 kHz. Normally, discrete versions of toothed whale clicks will only be 10-100 samples long, which either leads to derivation of the frequency spectrum on the basis of a much larger window or to a spectrum with very coarse frequency resolution. A smaller bin width on a short signal can at first glance be achieved through zero padding (interpolation), where the signal is extended by a number of samples with a value of zero, but the actual resolution has not improved. In figure 9 we have computed the power spectrum of the click displayed in figure 8. The spectral characteristics of the signal are quantified from a 256-point FFT window symmetrical around the peak of the click envelope (the absolute value of the Hilbert tranformed version of the signal). The peak frequency (f_p, kHz) is defined as the center frequency of the band with the highest amplitude of the spectrum. The centroid frequency (f_0, kHz) is defined as the point dividing the spectrum in halves of equal energy (Au, 1993), which is a much more robust measure of the frequency emphasis of a

broad band click than the peak frequency (Madsen et al., 2004). Delphinid clicks often have bimodal spectra with two peaks more than an octave apart, but with small and varying amplitude differences across the spectrum. For such clicks the peak frequency can come out very differently for similar clicks, whereas the centroid frequency is a much more robust measure that uses the power distribution as a function of frequency in the clicks. The bandwidth (*BW*) of the signals can be paramerized by the *–3 dB BW* (kHz) and *–10 dB BW* (kHz) and by the centralized root mean square bandwidth (*RMS-BW*, kHz) (Au, 1993), providing a measure of the spectral standard deviation around the centroid frequency (f_0) of the linear spectrum (figure 9). The RMS-BW can be used as a proxy for the frequency window over which the animal integrates both signal energy and noise (Møhl et al., 2003).

DI estimation

If we can assure that the same signal has been recorded both on and off the acoustic axis in known angles, this information may be used to assess the beam pattern (the acoustic intensity as a function of the angle to the acoustic axis). With no information on animal orientation relative the array, it must be assumed that the beam pattern is rotational symmetric, which is a reasonable approximation for most species measured to date (Au et al., 1986; Au et al., 1988; Zimmer et al., 2005, Beedholm and Møhl, 2006) with the exemption of Pseudorca (Au et al., 1995). Knowing the beam pattern given by the ASL as a function of off-axis angle we may calculate the transmission directionality index (DI). The DI quantifies the directionality of a signal, and is defined as the ratio between the source level intensity on the acoustic axis and the source level intensity of a hypothetical omni-directional sound source (where ASL = SL) radiating the same acoustic power as the sound source in question (Urick, 1983). A DI of 20 dB means that the source level is 20 dB higher than what would be obtained from an omnidirectional sound source emitting the same power. With the beam pattern of pressure (p) sampled and extrapolated at N number of angles v_1 to v_N, spaced Δv apart, the directivity index can be approximated by (Møhl et al. 2003):

$$\mathrm{DI} = 10\log(2/\sum_{i=1}^{N} p_i \sin(v_i \Delta v))$$

The angular spacing Δv should be reasonably small to obtain a good approximation of DI with this equation. A useful theoretical framework for modeling of radiation patterns of echolocation clicks is that of a circular piston (Au et al., 1978, Au, 1993). The sound transmission of a toothed whale forehead can be modeled by a flat piston of equivalent aperture with the same DI (Au, 1993), and the off-axis waveforms can be modeled with accuracy by convolving the on-axis waveform with the transfer function of a flat piston as a function of off-axis angle (Beedholm and Møhl, 2006). The beam pattern given by the pressure, p, as a function of off-axis angle (ϑ) can described by a first order Bessel function using the wave number *k* times the equivalent aperture radius *a (*Au, 1993; Zimmer et al., 2005):

$$P(ka\sin(\vartheta)) = P_0 \frac{2J_1(ka\sin(\vartheta))}{ka\sin(\vartheta)}$$

The broad band beam pattern can either be derived by integrating $P(ka\sin(\vartheta))$ with respect to frequency, or approximated with a pure tone signal at the centroid frequency of the radiated click in question. The problem of using a single tone approximation is that it leads to deep notches in the beam response that would never be generated for a broad band signal. The *ka* product ($(2x\pi/\lambda)xa$, where λ is the wavelength and *a* is the radius of the transmitter) is a measure of the relationship between the effective transmission aperture and the radiated wavelength (here approximated by the centroid frequency of the radiated click). This measure comes in handy when assessing the relationship between the half power beam width ($Beam_{-3dB}$), the frequency emphasis of the echolocation click and the effective size of transmitting anatomical structure.

For $ka >> 1$, which applies for known echolocating toothed whales, the DI can be approximated by (Urick, 1983):

$$\text{DI} \approx 20\log(ka)$$

And the half power beam width can be estimated as (Zimmer et al., 2005):

$$Beam_{-3dB} \approx 185^\circ / ka$$

Consequently, the half power beam width is linked to the DI by (Zimmer et al., 2005):

$$Beam_{-3dB} \approx 185^{\circ} \text{ x } 10^{-DI/20}$$

When estimating the equivalent aperture of a toothed whale sound projection system, the dimensions normally come out as being smaller than the physical dimensions of the nasal complex of the whale, and the equivalent aperture estimate is larger for larger animals (Au et al., 1978; Au et al., 1988; Au et al., 1995). However, it is far from evident how the functional morphology of the nasal complex leads to the observed radiation pattern, and there is at present no well founded rationale behind the notion that the toothed whale sound generator should behave as a flat piston in an infinite baffle. The piston model should therefore be seen as a helpful tool to approximate and predict radiation patterns from toothed whales, but not as a de facto paradigm that can be forced on all observed radiation patterns.

Other techniques

Since derivation of source parameters in principle only requires knowledge on the range and the orientation of a clicking toothed whale with respect to a single calibrated receiver, it is possible to acquire the needed information without the aid of arrays of real and/or virtual hydrophones. Two recently developed techniques using onboard tags have provided elegant ways to derive source parameter estimates of echolocating toothed whales. Multisensor, archival tags, called Dtags (Johnson and Tyack, 2004) record sound with 16 bit resolution and at sampling rates up to 192 kHz along with animal orientation parameterized by 3-axis accelerometers and magnetometers sampled at 50 Hz.

Zimmer et al. (2005a) used such an onboard tag in conjunction with a towed hydrophone system to derive source parameters of echolocation clicks from a tagged sperm whale. Knowing the depth of both the tagged whale and the towed hydrophone allowed for derivation of range between the whale and the receiver by exploiting multipath delays between the direct and surface reflected versions of the clicks. The relative

orientation of the whale with respect to the hydrophone in the far field was derived from the absolute pointing vector of the tagged whale and the depth and estimated GPS position of the towed hydrophone. This setup provided recordings of clicks in known aspects and ranges to the whale, generating the first 3-D radiation pattern of echolocation clicks from a toothed whale (Zimmer et al., 2005a).

In a second study with Dtags, Zimmer et al., (2005b) used the novel approach of having two tagged echolocating Cuviers beaked whales recording each other during deep foraging dives. Both animals were tagged with Dtags recording clicks of the tagged whale and clicks of nearby conspecifics, including the other tagged whale. The time delays between emission and reception of clicks from one whale to the other and vice versa allowed for derivation of the range between the two tagged whales (Johnson et al., in prep). The 3-axis orientation sensors of the tags provided the relative orientation of the whales for each click, which along with range between the whales allowed Zimmer et al., (2005b) to compute ASL as a function of off-axis angles. Subsequently, the off-axis angle versus ALS data provided the basis for estimating SL, DI and the spectral properties of the clicks. The advantage of having tagged animals recording each other is that they often dive to the same depth when foraging and that they stay fairly close together (Johnson et al., in prep). A possible bias is that they may try to avoid ensonifying each other with high sound pressure levels, which may lead to underestimation of the source parameters (Zimmer et al., 2005b) or that no on-axis clicks are recorded.

Acknowledgments

We dedicate this paper to Drs. Whitlow W. L. Au and Bertel Møhl who have pioneered quantitative recording and analysis of toothed whale echolocation clicks, and formulated many of the concepts presented in this paper. We are greatly indebted to M. Johnson, W.M.X. Zimmer, K. Beedholm, F. H. Jensen, B.K. Nielsen, J. Spiesberger and B. Møhl for helpful discussions and/or constructive critique on earlier versions of the manuscript. We also wish to acknowledge the skilled engineering contributions of N. U. Kristiansen. This work was supported by a Steno Fellowship from the Danish National Science Foundation to PTM, a grant from the Carlsberg Foundation to MW with additional support to the authors from Reson, the Novo Nordisk Science Foundation, Aarhus University Research Fund, and the Oticon Foundation.

References

Apel, J. R. 1987. Principles of ocean physics. Academic Press, New York.

Au W.W.L. (1993). Sonar of Dolphins, New York: Springer Verlag.

Au, W. W. L. (1997). Echolocation in Dolphins with a Dolphin-Bat Comparison. Bioacoustics 8, 162-185.

Au, W.W.L, Floyd, R.W., Penner, R.H., Murchison, A.E., (1974). Measurement of echolocation signals of the Atlantic bottlenose dolphin, Tursiops truncatus Montagu, in open waters. *J. Acoust. Soc. Am.* 56, 1280-1290.

Au W.W.L., Floyd R.W. and Haun J.E. (1978) Propagation of Atlantic bottlenose dolphin echolocation signals. J. Acoust. Soc. Am. 64: 411-422.

Au, W. W. L., J. L. Pawloski, P. E. Nachtigall, M. Blonz, R. C. Gisiner 1995. Echolocation signals and transmission beam pattern of a false killer whale (Pseudorca crassidens). J. Acoust. Soc. Am. 98(1): 51-59.

Au, W. W. L. 2004. Echolocation signals of wild dolphins. Acoustical Physics, vol. 50(4): 454-462.

Au & Benoit Bird, Nature paper on AGC

Au, W.W.L., Penner R.H., and Turl C.W. (1987) Propagation of beluga echolocation signals. J. Acoust. Soc. Am., 82: 807-813.

Au, W.W.L, Moore, P. W., and Pawloski, D. (1986). Echolocation transmitting beam of the Atlantic bottlenose dolphin. *J. Acoust. Soc. Am.* 80, 688-691.

Au, W.W.L. and Pawloski, D. A. (1989). A comparison of signal detection between an echolocating dolphin and an optimal receiver. *J. Comp. Physiol* [A] 164, 451-458.

Au, W.W.L, Pawloski,J.L., Nachtigall,P.E., Blonz,M., Gisner,R.C. (1995). Echolocation signals and transmission beam pattern of a false killer whale (Pseudorca crassidens). *J. Acoust. Soc. Am.* 98, 51-59.

Au, W.W.L. (1997). Echolocation in Dolphins with a Dolphin-Bat Comparison. *Bioacoustics* 8, 162.

Au, W.W.L., Ford, J.K.B, Horne, J.K. and Allman K.A.N. (2004) Echolocation signals of free-ranging killer whales (Orcinus orca) and modelling of foraging for chinook salmon (Oncorhyncus tswawytscha). *J. Acoust. Soc. Am.*, 115(2), 901-909.

Au, W.W.L. and Herzing, D. L. (2003). Echolocation signals of wild Atlantic spotted dolphin (Stenella frontalis). *J. Acoust. Soc. Am.*, 113, 598-604.

Au, W. W. L., Kastelein, R. A., Rippe, T., and Schooneman, N. M. (1999). "Transmission Beam Pattern and Echolocation Signals of a Harbor Porpoise (*Phocoena phocoena*)," J. Acoust. Soc.Am. 196, 3699-3705.

Au, W. W. L. and Benoit-Bird, K. J. (2003). Automatic gain control in the echolocation system of dolphins. Nature 423, 861-863.

Aubauer, R., M. O. Lammers, W. W. L. Au 2000. One-hydrophone method for estimating distance and depth of phonatic dolphins in shallow water. J. Acoust. Soc. Am. 107(5): 2744-2749.

Barlow, J., B. L. Taylor (2005). Estimates of sperm whale abuncance in the northeastern temperate Pacific from a combined acoustic and visual survey. Mar. Mamm Sci. 21(3): 429-445.

Beedholm, K., B. Møhl 2006. Directionality of sperm whale sonar clicks and its relation to piston radiation theory. J. Acoust. Soc. Am. 119(2): EL 14-EL19.

Cranford, T. W., Amundin, M., and Norris, K. S. (1996). Functional morphology and homology in the odontocete nasal complex: implications for sound generation. J.Morphol. 228, 223-285.

Diercks, K. J., R. T. Trochta, W. E. Evans 1973. Dolphin sonar: measurements and analysis. J. Acoust. Soc. Am. 54(1): 200-204.

Brill, R., Pawloski, J. L., Helweg, D., Au, W. W. L., and Moore, P. W., (1992)Target detection, shape discrimination and signal characteristics of an echolocating false killer whale (Pseudorca crassidens). *J. Acoust. Soc. Am.*, 92(3), 1324-1330.

Evans, W.E. (1973). Echolocation by Marine Delphinids and One Species of Freshwater Dolphin. *J. Acoust. Soc. Am.*, 54, 191-199.

Heerfordt, A., B. Møhl, M. Wahlberg 2006. A wideband connection to sperm whales: a fiber-optic deep-sea hydrophone array. Deep Sea Research, in press.

Johnson, M. P. and Tyack, P. L. (2003). A digital acoustic recording tag for measuring the response of wild marine mammals to sound. *IEEE Journal of Oceanic Engineering* 28, 3-12.

Laplance, C., O. Adam, M. Lopatka, J.-F. Motsch 2004. Depth/range localization of diving sperm whales using passive acoustics on a single hydrophone disregarding seafloor reflections. J. Acoust. Soc. Am. 119: 3403-.

Leaper, R., Chappell, O., and Gordon, J. C. D., (2002). "The development of practical techniques for surveying sperm whale populations acoustically," Rep. Int. Whal. Comm. 42, 549-560.

Levenson, C. 1974. Source level and bistatic target strength of the sperm whale (Physeter catodon) measured from an oceanographic aircraft. J. Acoust. Soc. Am. 55(5): 1100:1103.

Madsen, P. T., Payne, R., Kristiansen, N.U., Kerr, I., and Moehl, B. (2002a). Sperm whale sound production studied with ultrasound-time-depth-recording tags. *Journal of Experimental Biology* 205, 1899-1906.

Madsen, P. T., Wahlberg, M., and Møhl, B. (2002b). Male sperm whale (*Physeter macrocephalus*) acoustics in a high latitude habitat: implications for echolocation and communication. Behavioral Ecology and Sociobiology 53: 31-41.

Madsen, P. T., Kerr, I., and Payne, R. (2004a). Echolocation clicks of two free-ranging delphinids with different food preferences: false killer whales (*Pseudorca crassidens*) and Risso's dolphin (*Grampus griseus*). Journal of Experimental Biology 207, 1811-1823.

Madsen,P.T., Kerr,I., Payne,R., (2004b). Source parameter estimates of echolocation clicks from wild pygmy killer whales (*Feresa attenuata*) (L). J. Acoust. Soc. Am. 116, 1909-1912.

Madsen,P.T., Carder,D.A., Beedholm,K., Ridgway,S., 2005. Porpoise clicks from a sperm whale nose: convergent evolution of toothed whale echolocation clicks? Bioacoustics. 15: 195-206

Madsen, P.T. (2005), "Marine Mammals and Noise: What is a safety level of 180 dB re. 1uPa (rms) for transients?", J. Acoust. Soc. Am. 117(6): 3952-3957

Madsen, P. T., Johnson, M., Aguilar de Soto, N., Zimmer, W. M. X. and Tyack, P. L. (2005). Biosonar performance of foraging beaked whales (*Mesoplodon densirostris*). The Journal of Experimental Biology 208, 181-194.

Medwin, H. and Clay, C.S. (1998). Acoustical Oceanography. Boston, Academic press.

Miller, L. A., Pristed, J., Moehl, B. and Surlykke A. (1995). Click sounds from narhwals (*Monodon monoceros*) in Inglefield Bay, Northwest Greenland. Marine Mammal Science 11, 491-502.

Murchison A.E.1980 Maximum detection range and range resolution in echolocating bottlenose porpoise (Tursiops truncatus) In: R.G. Busnel and J.F. Fish eds Animal Sonar Systems NY Plenum Press: 43-70

Møhl, B., Surlykke, A., and Miller, L. A. (1990). High Intensity Narwhal Click. In: *Sensory Abilities of Cetaceans* (eds. Thomas, J. and Kastelein, R.), pp. 295-304. New York: Plenum Press.

Møhl, B., Wahlberg, M., Madsen, P. T., Miller, L. A., and Surlykke, A., (2000). "Sperm whale clicks: directionality and source level revisited," J. Acoust. Soc. Am. 107, 638-648.

Møhl, B., M. Wahlberg, A. Heerfordt (2001). A large-aperture array of nonlinked receivers for acoustic positioning of biological sound sources. J. Acoust. Soc. Am. 109(1): 434-437.

Møhl, B., Wahlberg, M., Madsen, P.T., Heerfordt, and Lund, A. (2003). The monopulsed nature of sperm whale clicks. J. *Acoust. Soc. Am.* 114, 1143-1154.

Rasmussen, M. H., Miller, L. A., and Au, W.W.L. (2002). Source levels of clicks from free-ranging white-beaked dolphins (Lagenorhynchus albirostris Gray 1846) recorded in Icelandic waters. *J. Acoust. Soc. Am.*, 111, 1122-1125.

Rasmussen, M., M. Wahlberg, L. A. Miller (2004). Estimating transmission beam pattern of clicks recorded from free-ranging white-beaked dolphins (Lagenorhynchus albirostris). J. Acoust. Soc. Am. 116(3): 1826-1831.

Roitblat, H. L., Helweg, D., and Harley, H. E. (1995). Echolocation and imagery. In: *Sensory systems of aquatic mammals* (eds. Kastelein, R., Thomas, J., and Helweg, D.), pp. 171-181. Woerden: De Spil Publishers.

Rhinelander, M. Q., and Dawson, S. M. (2004). "Measuring sperm whales from their clicks: Stability of interpulse intervals and validation that they indicate whale length,'' J. Acoust. Soc. Am. 115, 1826–1831.

Richardson,W.J., Greene,C.R., Jr., Malme,C.I., Thomson,D.H., 1995. Marine Mammals and Noise, Academic Press, London.

Schotten, M., Au,W.W.L., Lammers,M.O., Aubauer,R., (2003). Echolocation recordings and localizations of wild spinner dolphins (*Stenella longirostris*) and pantropical spotted dolphins (*Stenella attenuata*) using a four hydrophone array. In: *Echolocation in bats and dolphins* (eds. Thomas, J., Moss, C. F., and Vater, M.), Chicago: University of Chicago Press.

Spiesberger, J. L. and Fristrup, K. M. (1990). Passive Localization of Calling Animals and Sensing of Their Acoustic Environment Using Acoustic Tomography. *American Naturalist* 135, 107-153.

Spiesberger, J. L. 2001. Hyperbolic location errors due to insufficient numbers of receivers. J. Acoust. Soc. Am. 109(6): 3076-3079.

Spiesberger, J. L. 2005. Probability distributions for locations of calling animals, receivers, sound speeds, winds, and data from travel time differences. J. Acoust. Soc. Am.

Spiesberger, J. L., M. Wahlberg 2002. Probability density functions for hyperbolic and isodiachronic locations. J. Acoust. Soc. Am. 112(6): 3046-3052.

Surlykke, A. and Moss, C. F. (2000). Echolocation behavior of big brown bats, Eptesicus fuscus, in the field and the laboratory. *J. Acoust. Soc. Am.* 108, 2419-2429.

Thode, A., Mellinger, D. K., Stienessen, S., Martinez, A., and Mullin, K. (2002). "Depth-dependent acoustic features of diving sperm whales (*Physeter macrocephalus*) in the Gulf of Mexico," J. Acoust. Soc. Am., 112(1), 308-321.

Urick, R. J. (1983). Principles of underwater sound. Los Altos, Peninsula Publishing.

Wahlberg, M., Møhl, B., and Madsen, P.T. (2001). Estimating source position accuracy of a larger-aperture hydrophone array for bioacoustics. *J. Acoust. Soc. Am.* 109(1), 397-406.

Wahlberg, M. (2002). "The acoustic behaviour of diving sperm whales observed with a hydrophone array," J. Exp. Mar. Biol. Ecol., 281, 53-62.

Wahlberg M. (2003). Comparing a linear with a non-linear technique for acoustic localization of right whales. Canadian Acoustics 32(2): 125-131.

Wenz G (1962) Acoustic ambient noise in the ocean: spectra and sources. J. Acoust. Soc. Am. 34(12): 1936-1956

Watkins, W. A. (1980). Click sounds from animals at sea. In: *Animal Sonar Systems* (eds. Busnel, R. G. and Fish, J. F.), pp. 291-298.

Watkins, W. A. and Daher, M.A. (1992) Underwater sound recording of animals. *Bioacoustics* 4, 195-209.

Watkins, W. A. and Schevill, W.E. (1972). Sound source location by arrival-times on a non-rigid three-dimensional hydrophone array. *Deep-Sea Rese*arch 19, 691-706.

Weber, P. J.(1963). The tape recorder as an instrumentation device, Ampex Corporation.

Woodward,P.M., 1953. Probability and information theory with application to radar, Pergamon Press, NY.

Young,R.W., 1970. On the energy transported with a sound pulse. Journal Of The Acoustical Society Of America 47, 441-442.

Zimmer, W.M.X., Tyack, P.L., Johnson, M.P., Madsen, P.T., (2005). "Three-dimensional beam pattern of regular sperm whale clicks confirms bent-horn hypothesis". The Journal of the Acoustical Society of America 117, 1473-1485

Zimmer,W.M.X., Johnson,M., Madsen,P.T., Tyack,P., 2005. Echolocation clicks of free-ranging Cuviers beaked whales (Ziphius cavirostris). Journal Of The Acoustical Society Of America 117, 3919-3927.

Table I. Summary of array types. N_r: number of receivers, MINNA: minimal receiver number array, ODA: Over-determined array. $N_{coordinates}$ indicates the number of source coordinates that are possible to derive with the array. In the first column, circles indicate receivers in the horizontal plain, bold circles are located in a different vertical coordinate. Parenthesis around examples of coordinates indicates that the coordinates may be ambiguous, e.g. when the source may be located on either side of the array plane.

	N_r	Geometry	Array name	$N_{coordinates}$	Examples
o	1	Point	single	-	-
oo	2	Line	stereo	1	(bearing)
ooo	3	Line	linear	2	(x, y), range
o **o o**	3	Plane	2-D MINNA	2	(x, y, bearing, range)
o o o **o o oo**	>3	Plane	2-D ODA, or 2/3-D	>2	x, y, (z, bearing, range)
o o o **o**	4	Volume	3-D MINNA	3	(x,y,z, bearing, range)
o o **oo o o**o	>4	Volume	3-D ODA	>3	x,y,z, bearing, range

Figure 1

A) Radiation pattern of a click from an echolocating dolphin (Au, 1993) showing off axis distortion. B) The passive sonar equation applied to a clicking dolphin. SL is the back calculated sound pressure level (Received level (RL) + transmission loss (TL)) one meter from the source and on the acoustic axis. ASL is the sound pressure back calculated to 1 meter in an unknown aspect to the animal.

Figure 2

Modelling the received level of a harbour porpoise click emitted at 1 m depth and received at 5 m depth at different ranges. Bottom depth is 10 m. The dotted line indicates a transmission loss according to spherical spreading and absorption of 38 dB/km. The model does not take into account that the signal is directional, so the effect of surface interference may be somewhat exaggerated.

Figure 3

Clicking dolphin and a recording chain with a hydrophone, an amplifier and an analog-to-digital-converter (ADC). The dolphin produces an analog pressure waveform that is converted to an analog voltage waveform by the hydrophone. The amplifier unit filters and amplifies the analog voltage input before digitization in the ADC that forms a discrete version of the click.

Figure 4

A) Sensitivity of a spherical hydrophone (Reson TC4043) as a function of frequency. Note that it is reasonably flat up to the resonance frequency of the element around 120 kHz. B) Receiving directivity in the horizontal plane of the same hydrophone. C) Receiving directivity in the vertical plane of the same hydrophone.

Figure 5

Localizing a dolphin with a 4-hydrophone linear array. The time-of-arrival differences at the receivers (marked with circles) generate three independent hyperbolas. They do not intersect in a single point, due localization errors as described in the text. The analytical source location (see appendix) is marked with a star and lies within the hyperbola crossings.

Figure 6.

Maximum error in calculated transmission loss for a harbour porpoise signal (sloping lines) and a sperm whale (almost horizontal lines) located at a range of up to 100 m distance, with a ranging absolute error of 10 and 20%, corresponding to received level errors of 1-2 dB when only considering spherical spreading.

Figure 7

Modelling the source localization error for a 4-hydrophone array, assuming a good signal-to noise ratio on all four receivers. The sound velocity is assumed to be known within 10 m/s, the receiver locations within 5 mm, and the TOADs are assumed to be measurable within 10 μs. The errors are given in units of percentage error (calculated as the average error out of 100 simulations) relative the range to receiver 1 (the top receiver). Receivers are denoted with filled circles. The figure does not take into account any erroneous horizontal shift in receiver locations (array bending).

Figure 8

A) Toothed whale click as received by the hydrophone. B) Discrete version of the click in A) sampled at 500 ksamples/sec. C) Cumulated relative energy in the interpolated (10 times) waveform of B) to define 95% duration (dotted lines). D) Peak-peak and rms measures computed on the discrete version of the click in A).

Figure 9

Power spectrum generated from 256 size FFT. Binwidth of 2 kHz. Fc = centroid frequency, Fp = peak frequency, RMSc-BW = centralized root-mean-square band width.

Appendix 1

```
% Source localization and hyperbola plot with linear array implemented in Matlab
% M Wahlberg, Aarhus University, April 2006
%
clear;
c0 = 1494.;                             % speed of sound (m/s)
R = -4 - [0 2 4 6 ]';                   % receiver depth coordinate (m)
t= [-0.1657   -0.1657  0]'*10^-3;        % TOADs for receiver 2 -receiver 1 and so on, see Wahlberg et al. 2001 and this ms
r = (R(2:end)-R(1));                    % normalized receiver coordinates
step = .01;                             % step size in hyperbola plots
A = 2 * [r t*c0^2];                     % source location A matrix, defined in Wahlberg et al. 2001 and this ms
b = - (t.^2)*(c0^2) + r.^2;             % source location b column vector, defined in Wahlberg et al. 2001 and this ms
m = A\b;                                % source solution solved by least squares as in Wahlberg et al. 2001 and this ms
so(2) = m(1)+R(1);                      % source depth coordinate
so(1) = sqrt((c0*m(2))^2 - m(1)^2 );    % source horizontal coordinate
figure(1); set(1,'Color',[1 1 1]);
plot(zeros(4,1),R,'ko');                % plot receivers
ax = [-3 2*so(1) min([so(2) min(R)])-5  max([ so(2) max(R) ])+5];   % define size of plot
hold on
plot(so(1),so(2),'r*');                 % plot source coordinates
for i=1:length(r),
    a = c0*t(i)/2;                      % the three parameters a, b, and c used to define the hyperbola curve in line 29
    c = r(i) / 2;
    b = sqrt(c^2 - a^2);
    if imag(b) == 0,                    % check if TOAD render physical hyperbola
        if t(i) ~= 0
            y = -sign(r(i))*sign(t(i))*[step:step:2*(ax(4)-ax(3))] ;  % equally spaced vector for which to calcualate a hyperbola below
            x = b * sqrt( y.^2 / a^2 - 1); % equation of a hyperbola curve with the parameters a and b defined above
        else
            y = zeros(1,2);             % plot straight line instead if TOAD is zero
            x = [0 ax(2)];
        end
        ind = min(find(imag(x)==0));    % find index in x vector where hyperbola starts
        x = [ fliplr(-x(ind:end)) x(ind:end) ]'; % extend hyperbola to both positive and negative x values
        y = [ fliplr(y(ind:end))  y(ind:end)]' + c + R(1); % estend y vector to two-sided hyperbola curve
        plot(x,y)                       % plot hyperbola
    end
end
axis(ax);
xlabel('Range (m)');
ylabel('Depth (m)');
% End of program
```

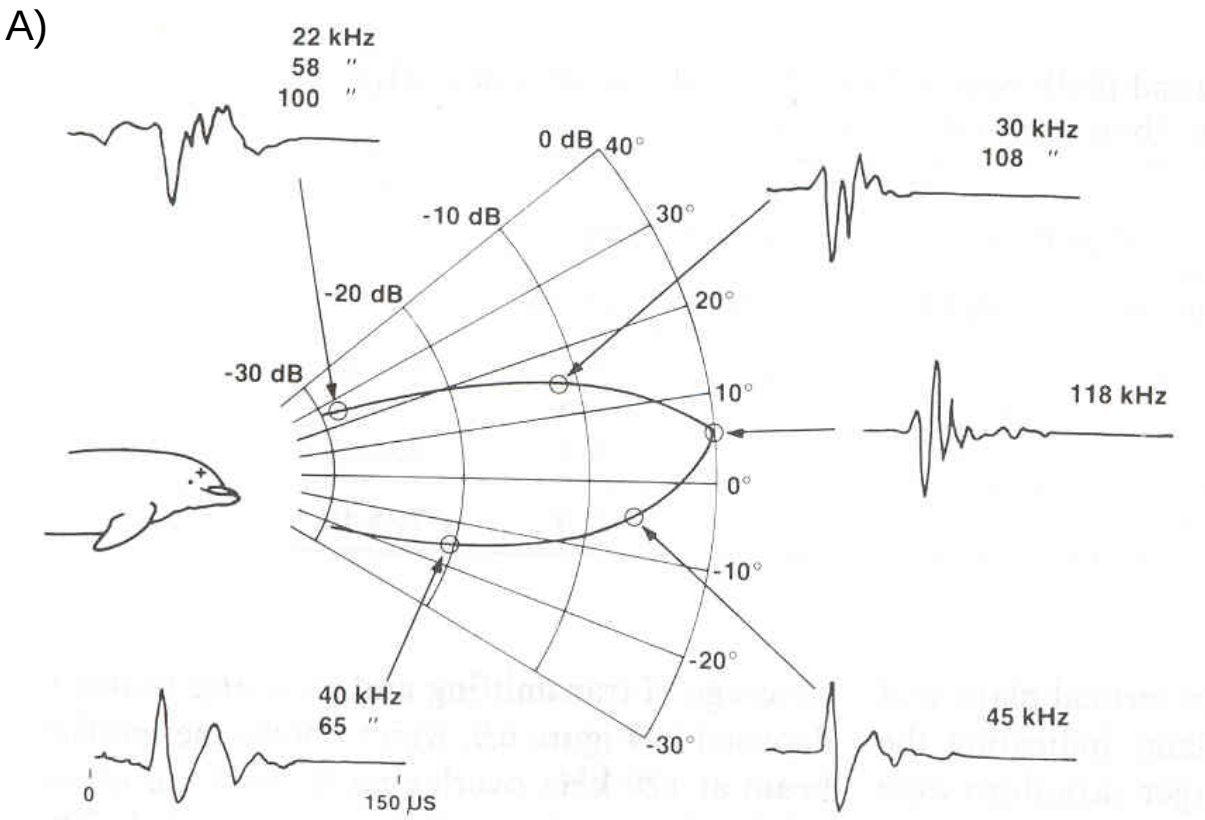
A)
22 kHz
58 "
100 "
0 dB
40°
30°
20°
10°
0°
-10°
-20°
-30°
-10 dB
-20 dB
-30 dB
30 kHz
108 "
118 kHz
45 kHz
40 kHz
65 "
0
150 µS

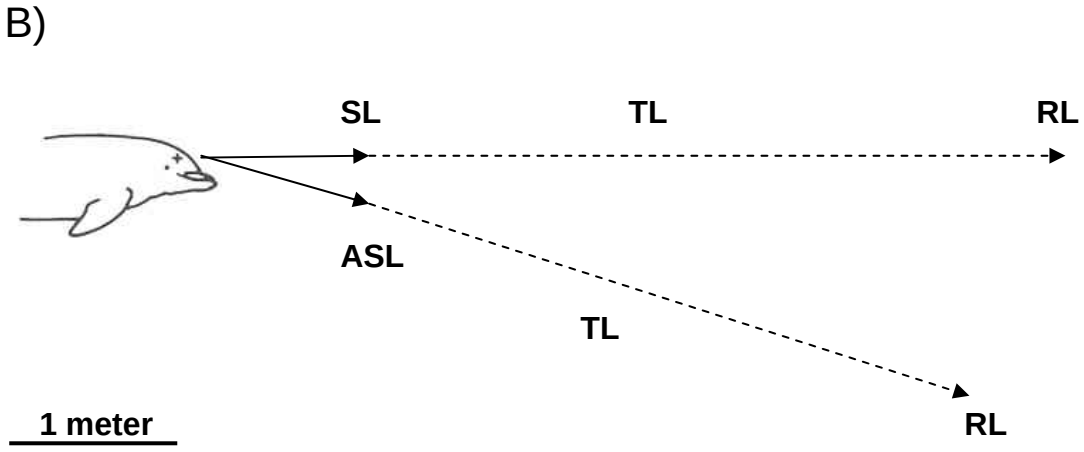
B)
SL
TL
RL
ASL
TL
1 meter
RL

Figure 1

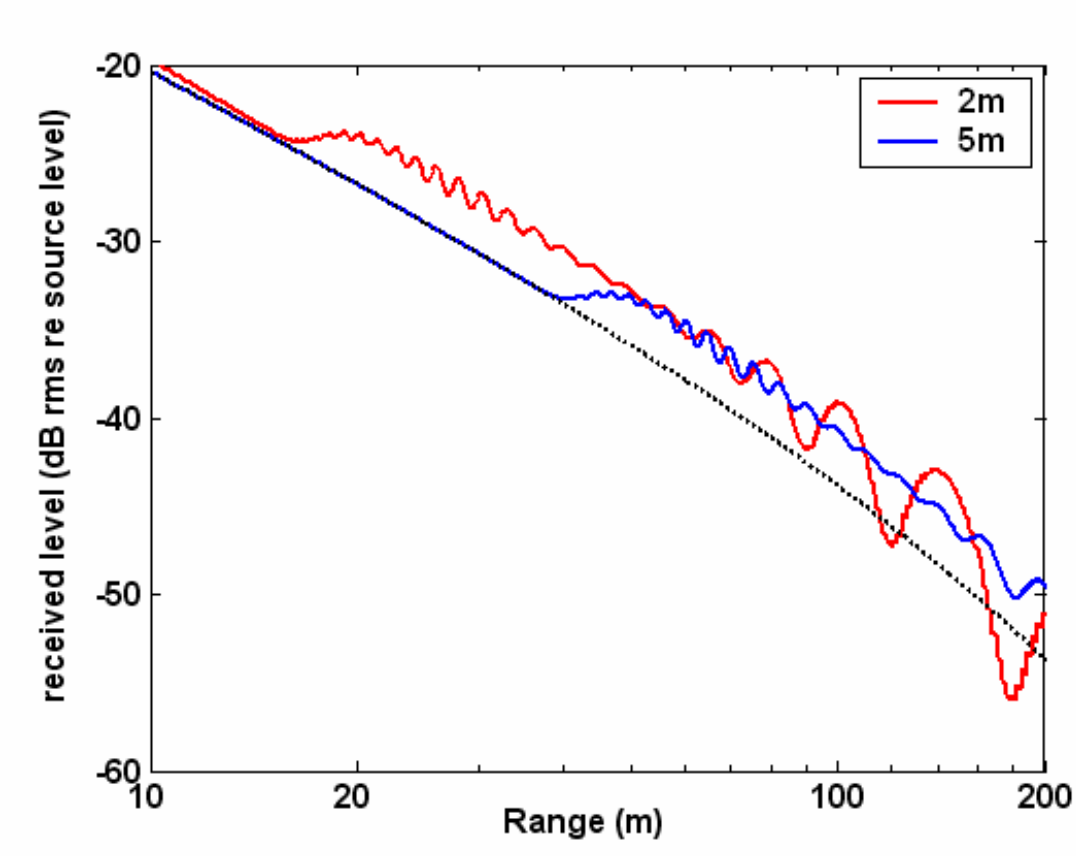
-20
-30
-40
-50
-60
10
20
100
200
Range (m)
received level (dB rms re source level)
2m
5m

Figure 2

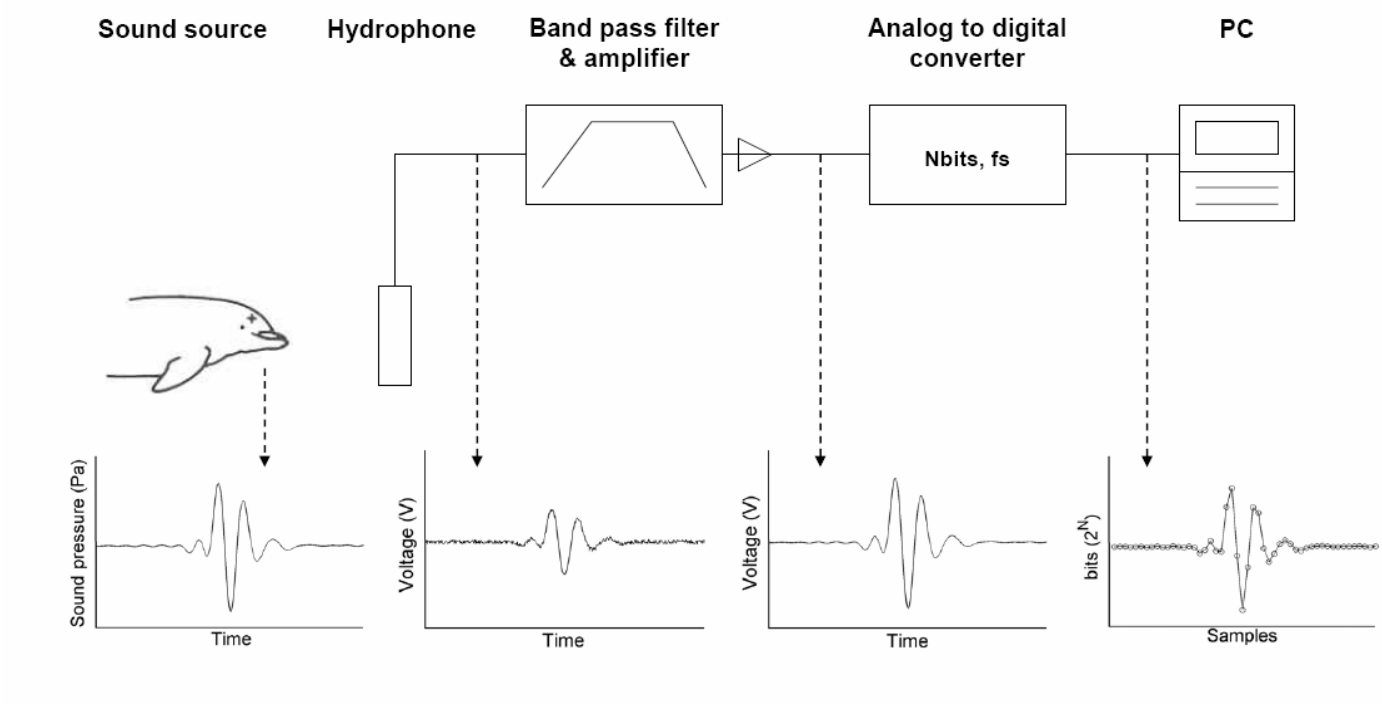
Sound source
Hydrophone
Band pass filter & amplifier
Analog to digital converter
PC
Nbits, fs
Sound pressure (Pa)
Time
Voltage (V)
Time
Voltage (V)
Time
bits (2^N)
Samples

Figure 3

A)

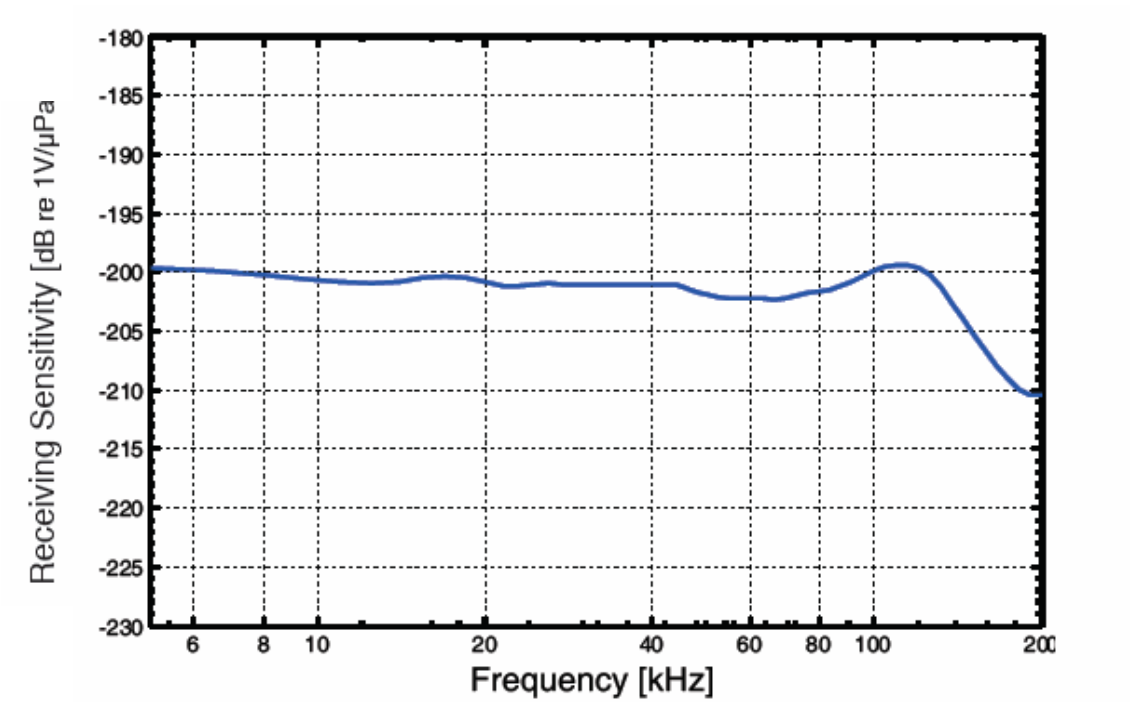
Receiving Sensitivity [dB re 1V/µPa
-180
-185
-190
-195
-200
-205
-210
-215
-220
-225
-230
6
8
10
20
40
60
80
100
200
Frequency [kHz]

B)

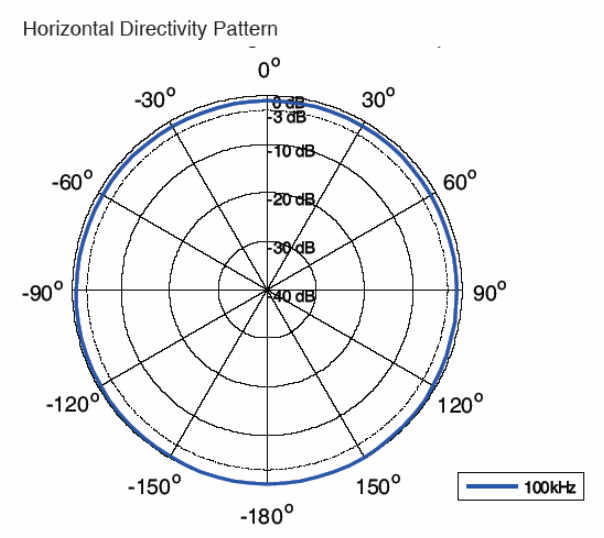
Horizontal Directivity Pattern
0°
30°
60°
90°
120°
150°
-180°
-150°
-120°
-90°
-60°
-30°
0 dB
-3 dB
-10 dB
-20 dB
-30 dB
-40 dB
100kHz

C)

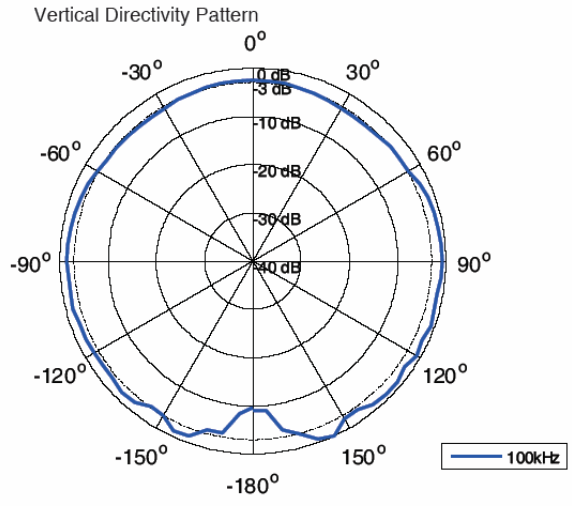
Vertical Directivity Pattern
0°
30°
60°
90°
120°
150°
-180°
-150°
-120°
-90°
-60°
-30°
0 dB
-3 dB
-10 dB
-20 dB
-30 dB
-40 dB
100kHz

Figure 4

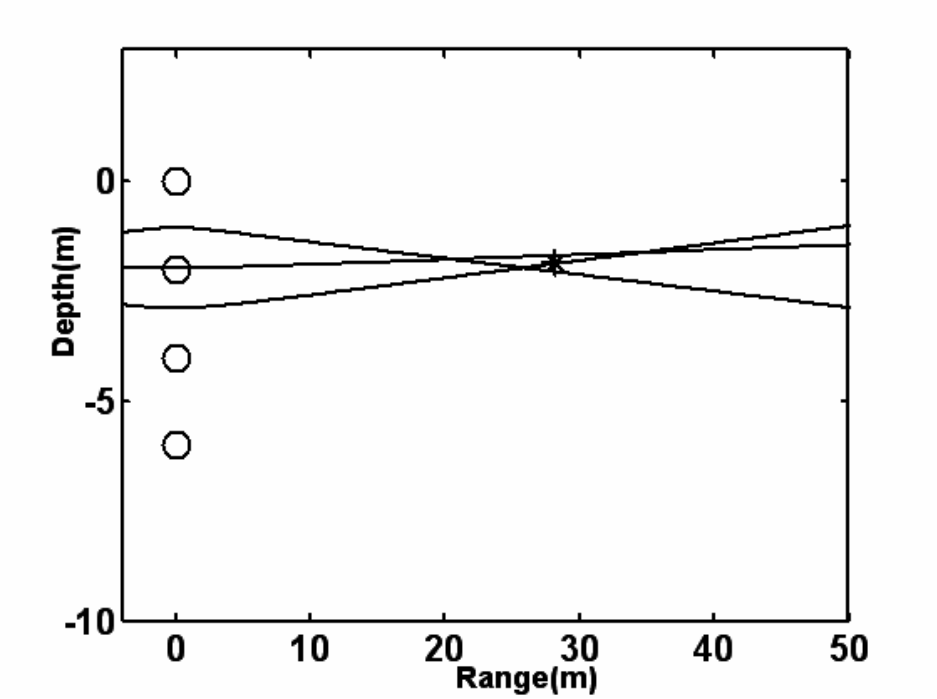

Figure 5

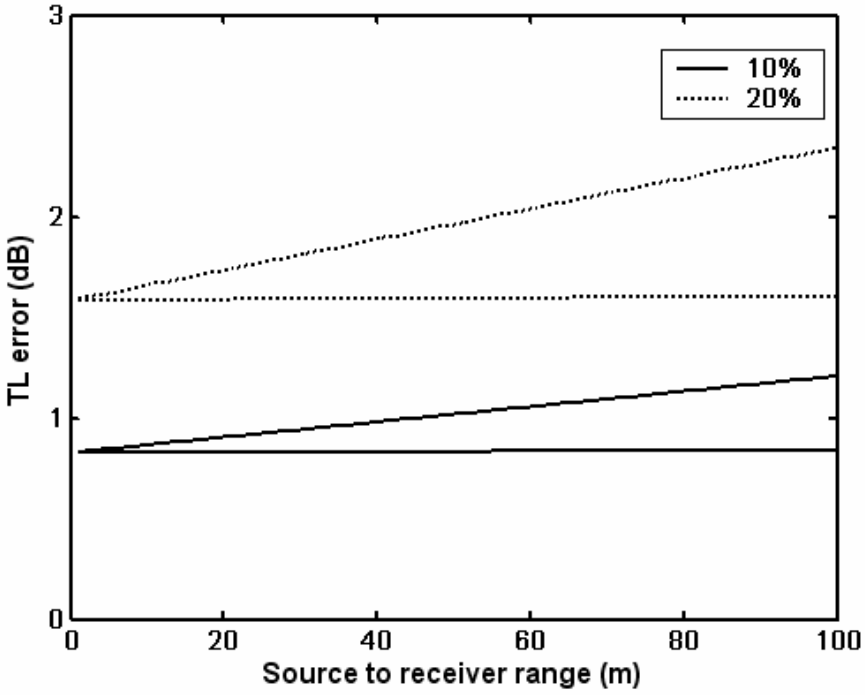
10%
20%
TL error (dB)
Source to receiver range (m)
0
1
2
3
0
20
40
60
80
100

Figure 6

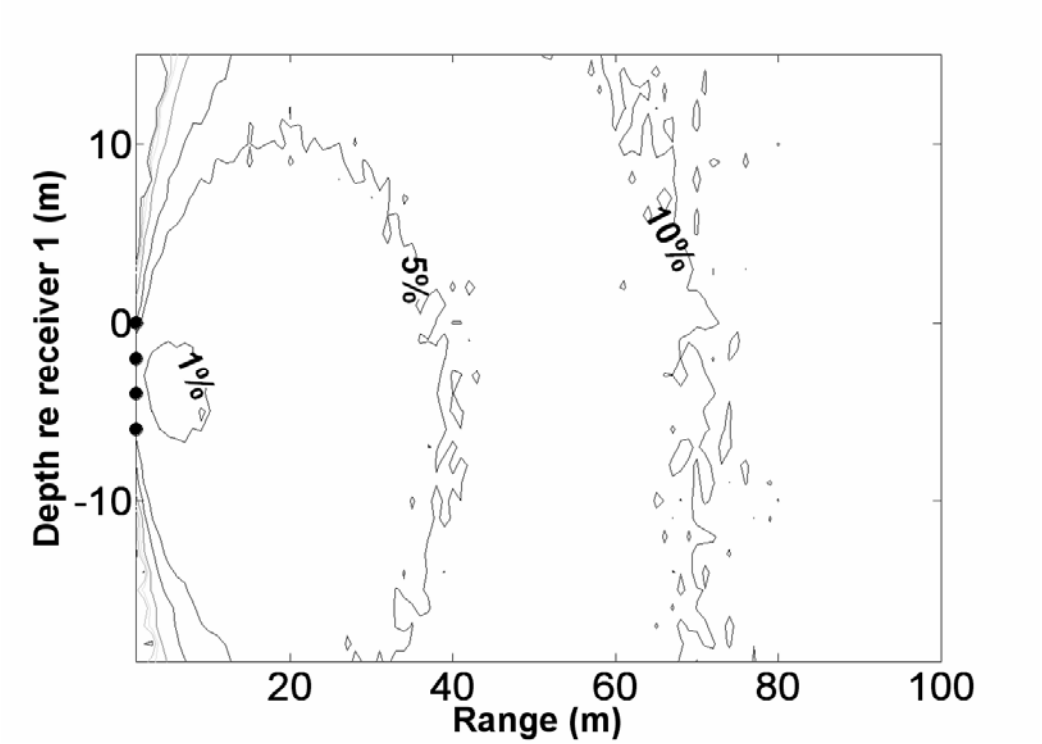

Figure 7

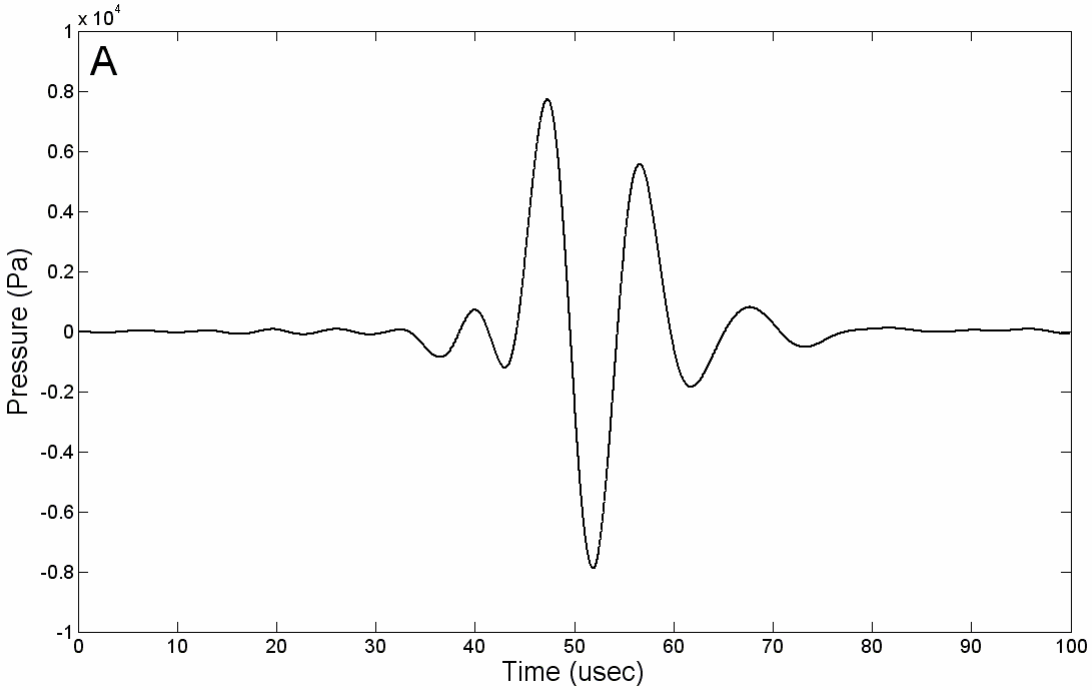
A
x 10^4
1
0.8
0.6
0.4
0.2
0
-0.2
-0.4
-0.6
-0.8
-1
Pressure (Pa)
0
10
20
30
40
50
60
70
80
90
100
Time (usec)

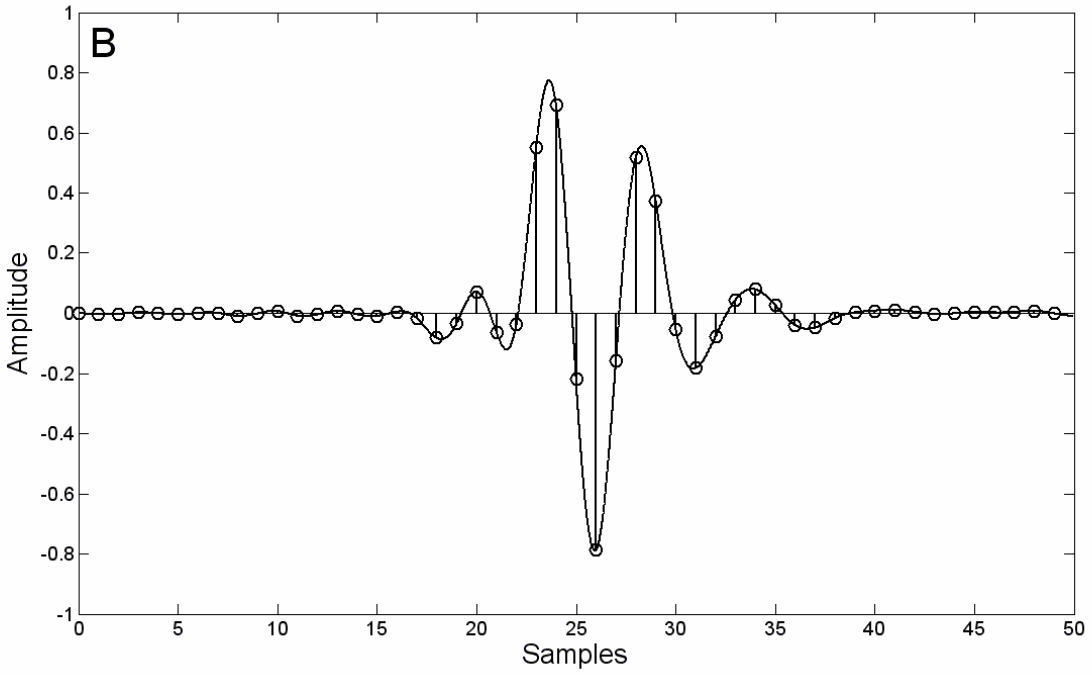
B
1
0.8
0.6
0.4
0.2
0
-0.2
-0.4
-0.6
-0.8
-1
Amplitude
0
5
10
15
20
25
30
35
40
45
50
Samples

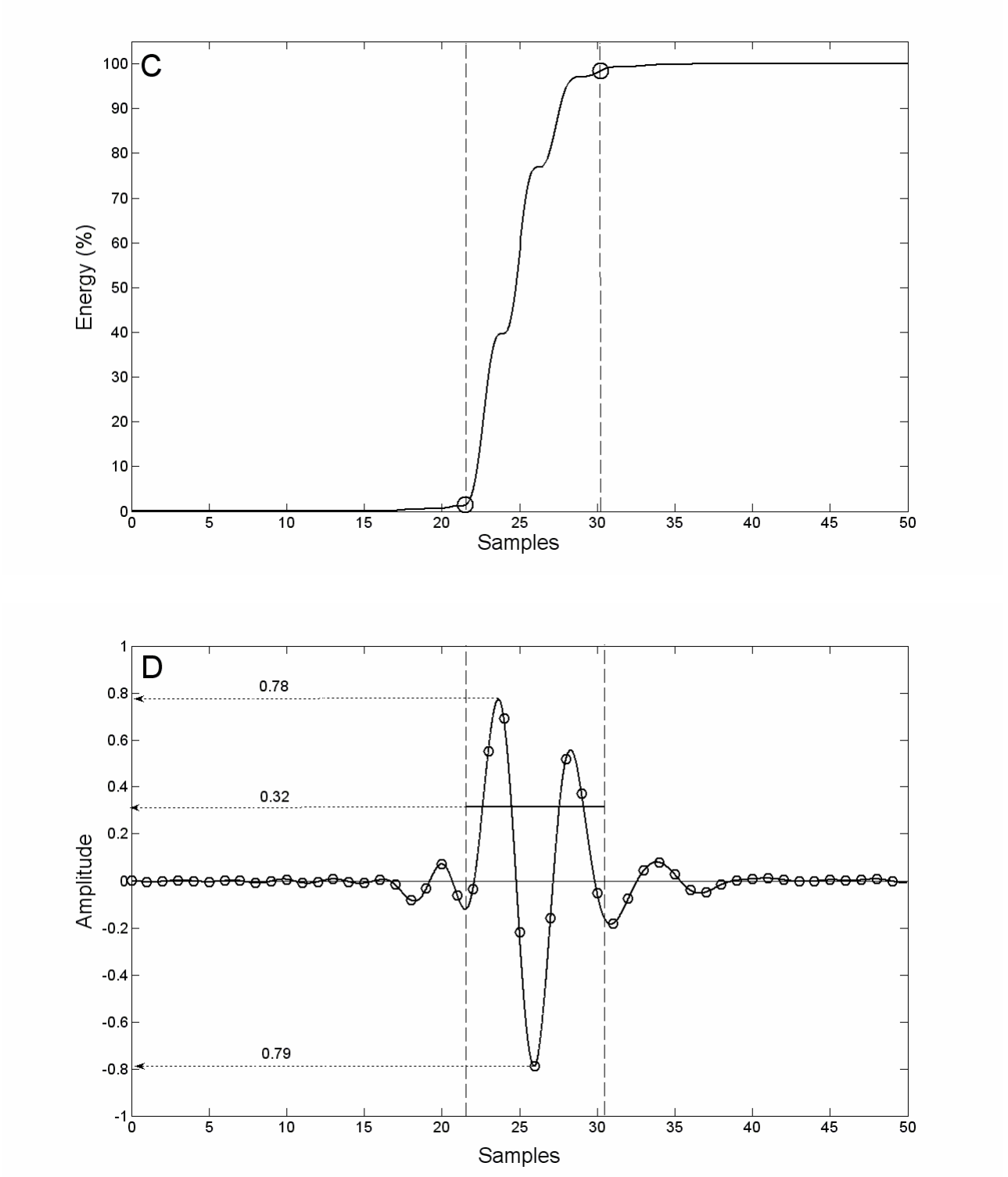

Figure 8

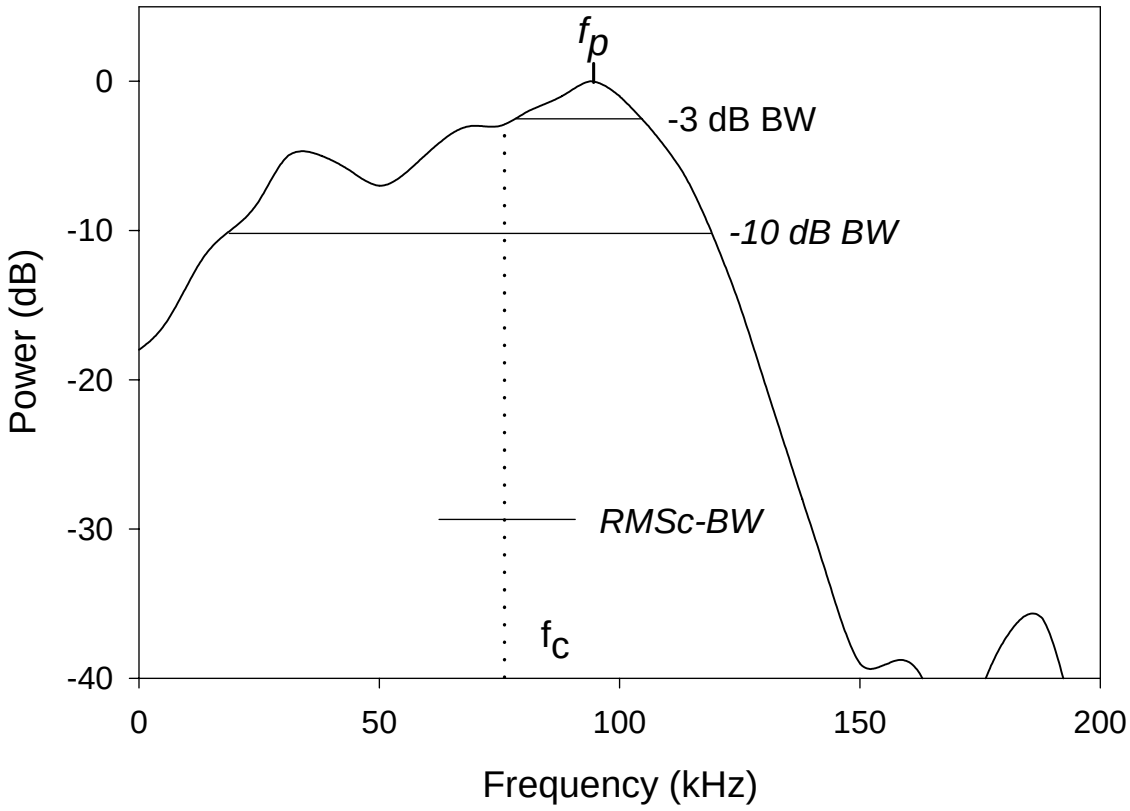
f_p
-3 dB BW
-10 dB BW
RMSc-BW
f_c
0
-10
-20
-30
-40
Power (dB)
0
50
100
150
200
Frequency (kHz)

Figure 9